

1 **Exploring the impact of forcing error characteristics on physically based snow** 2 **simulations within a global sensitivity analysis framework**

3

4 **M.S. Raleigh¹, J.D. Lundquist² and M.P. Clark¹**

5 [1] National Center for Atmospheric Research, Boulder, Colorado, USA

6 [2] Civil and Environmental Engineering, University of Washington, Seattle, Washington, USA

7 Correspondence to: M.S. Raleigh (raleigh@ucar.edu)

8

9 **Abstract**

10 Physically based models provide insights into key hydrologic processes, but are associated with
11 uncertainties due to deficiencies in forcing data, model parameters, and model structure. Forcing
12 uncertainty is enhanced in snow-affected catchments, where weather stations are scarce and
13 prone to measurement errors, and meteorological variables exhibit high variability. Hence, there
14 is limited understanding of how forcing error characteristics affect simulations of cold region
15 hydrology and which error characteristics are most important. Here we employ global sensitivity
16 analysis to explore how (1) different error types (i.e., bias, random errors), (2) different error
17 probability distributions, and (3) different error magnitudes influence physically based
18 simulations of four snow variables (snow water equivalent, ablation rates, snow disappearance,
19 and sublimation). We use Sobol' global sensitivity analysis, which is typically used for model
20 parameters, but adapted here for testing model sensitivity to co-existing errors in all forcings.
21 We quantify the Utah Energy Balance model's sensitivity to forcing errors with 1 840 000 Monte
22 Carlo simulations across four sites and five different scenarios. Model outputs were (1)
23 consistently more sensitive to forcing biases than random errors, (2) generally less sensitive to
24 forcing error distributions, and (3) critically sensitive to different forcings depending on the
25 relative magnitude of errors. For typical error magnitudes found in areas with drifting snow,
26 precipitation bias was the most important factor for snow water equivalent, ablation rates, and
27 snow disappearance timing, but other forcings had a more dominant impact when precipitation
28 uncertainty was due solely to gauge undercatch. Additionally, the relative importance of forcing
29 errors depended on the model output of interest. Sensitivity analysis can reveal which forcing
30 error characteristics matter most for hydrologic modeling.

31

32 **1. Introduction**

33 Physically based models allow researchers to test hypotheses about the role of specific processes
34 in hydrologic systems and how changes in environment (e.g., climate, land cover) may impact
35 key hydrologic fluxes and states (Barnett et al., 2008; Clark et al., 2011b; Deems et al., 2013;
36 Leavesley, 1994). Due to the complexity of processes represented, these models usually require
37 numerous meteorological forcing inputs and model parameters. Most inputs are not measured at
38 the locations of interest and require estimation; hence, large uncertainties may propagate from
39 hydrologic model inputs to outputs. Despite ongoing efforts to quantify forcing uncertainties
40 (e.g., Bohn et al., 2013; Clark and Slater, 2006; Flerchinger et al., 2009) and to develop
41 methodologies for incorporating uncertainty into modeling efforts (e.g., He et al., 2011b;
42 Kavetski et al., 2006a; Kuczera et al., 2010; Slater and Clark, 2006), many analyses continue to
43 ignore uncertainty. These often assume either that all forcings, parameters, and structure are
44 correct (Pappenberger and Beven, 2006) or that only parametric uncertainty is important (Vrugt
45 et al., 2008b). Neglecting uncertainty in hydrologic modeling reduces confidence in hypothesis
46 tests (Clark et al., 2011b), thereby limiting the usefulness of physically based models.

47

48 There are fewer detailed studies focusing on forcing uncertainty relative to the number of
49 parametric and structural uncertainty studies (Bastola et al., 2011; Benke et al., 2008; Beven and
50 Binley, 1992; Butts et al., 2004; Clark et al., 2008, 2011b, 2015a, 2015b; Essery et al., 2013;
51 Georgakakos et al., 2004; Jackson et al., 2003; Kuczera and Parent, 1998; Liu and Gupta, 2007;
52 Refsgaard et al., 2006; Slater et al., 2001; Smith et al., 2008; Vrugt et al., 2003a, 2003b, 2005;
53 Yilmaz et al., 2008). Di Baldassarre and Montanari (2009) suggest that forcing uncertainty has
54 attracted less attention because it is “often considered negligible” relative to parametric and
55 structural uncertainties. Nevertheless, forcing uncertainty merits more attention in some cases,
56 such as in snow-affected watersheds where meteorological and energy balance measurements are
57 scarce (Bales et al., 2006; Raleigh, 2013; Schmucki et al., 2014) and prone to errors due to
58 environmental or instrumental factors (Huwald et al., 2009; Lundquist et al., 2015; Rasmussen et
59 al., 2012). Forcing uncertainty is enhanced in complex terrain where meteorological variables
60 exhibit high spatial variability (Feld et al., 2013; Flint and Childs, 1987; Herrero and Polo, 2012;

61 Lundquist and Cayan, 2007). As a result, the choice of forcing data can yield substantial
62 differences in calibrated model parameters (Elsner et al., 2014) and in modeled hydrologic
63 processes, such as snowmelt and evapotranspiration (Mizukami et al., 2014; Wayand et al.,
64 2013). Thus, forcing uncertainty demands more attention in snow-affected watersheds.

65
66 Previous work on forcing uncertainty in snow-affected regions has yielded basic insights into
67 how forcing errors propagate to model outputs and which forcings introduce the most uncertainty
68 in specific outputs. However, these studies have typically been limited to: (1)
69 empirical/conceptual models (He et al., 2011a, 2011b; Raleigh and Lundquist, 2012; Shamir and
70 Georgakakos, 2006; Slater and Clark, 2006), (2) errors for a subset of forcings (e.g., precipitation
71 or temperature only) (Burles and Boon, 2011; Dadic et al., 2013; Durand and Margulis, 2008;
72 Lapo et al., 2015; Xia et al., 2005), (3) model sensitivity to choice of forcing parameterization
73 (e.g., longwave) without considering uncertainty in parameterization inputs (e.g., temperature
74 and humidity) (Guan et al., 2013), and (4) simple representations of forcing errors (e.g., Kavetski
75 et al., 2006a, 2006b). The last is evident in studies that only consider single types of forcing
76 errors (e.g., bias) and single distributions (e.g., uniform), and examines errors separately (Burles
77 and Boon, 2011; Koivusalo and Heikinheimo, 1999; Raleigh and Lundquist, 2012; Xia et al.,
78 2005). Lapo et al. (2015) show that biases have a greater impact than random errors on modeled
79 snow water equivalent and surface temperature, but this analysis only considers longwave and
80 shortwave forcings and considers errors separately. Examining uncertainty in one factor at a
81 time remains popular but fails to explore the uncertainty space adequately, ignoring potential
82 interactions between forcing errors (Saltelli and Annoni, 2010; Saltelli, 1999). In contrast,
83 global sensitivity analysis explores the uncertainty space more comprehensively by considering
84 uncertainty in multiple factors at the same time.

85
86 The purpose of this paper is to use global sensitivity analysis to assess how specific forcing error
87 characteristics influence outputs of a physically based snow model. To our knowledge, no
88 previously published study has investigated this topic in snow-affected regions. It is unclear how
89 (1) different error types (bias vs. random errors), (2) different error distributions, and (3)
90 different error magnitudes across all forcings affect model output. The impact of forcing errors

91 on models can be tested by corrupting forcings with specified characteristics (e.g., artificial
92 biases and random errors) and quantifying the impact on model outputs (e.g., Oudin et al., 2006;
93 Spank et al., 2013), but we are unaware of any detailed studies that have done this type of
94 experiment for all meteorological forcings commonly required for physically based snow
95 models. We hypothesize that (1) model outputs are more sensitive to biases than random errors
96 in forcing variables, (2) the assumed probability distribution for biases will alter the relative
97 ranking of importance in forcing errors, and (3) the magnitude of forcing biases will have a
98 strong influence on which forcing errors are most important.

99

100 In our view, it is important to clarify the relative impact of specific error characteristics on
101 modeling applications, so as to prioritize future research directions, improve understanding of
102 model sensitivity, and to address questions related to network design. For example, given budget
103 constraints, is it better to invest in a heating apparatus for a radiometer (to minimize bias due to
104 frost formation on the radiometer dome) or in a higher quality radiometer (to minimize random
105 errors associated with measurement precision)? Additionally, it is important to contextualize
106 different meteorological data errors, as these errors are usually studied independently of each
107 other (e.g., longwave radiation, Flerchinger et al., 2009; air temperature, Huwald et al., 2009),
108 and it is unclear how they compare in terms of model sensitivity.

109

110 The overarching research question is “how do assumptions regarding forcing error characteristics
111 impact our understanding of uncertainty in physically based model output?” Using the Sobol’
112 (1990) global sensitivity analysis framework, we investigate how artificial errors introduced into
113 high-quality observed forcings (temperature, precipitation, wind speed, humidity, shortwave
114 radiation, and longwave radiation) at four sites in contrasting snow climates propagate to four
115 snow model outputs (peak snow water equivalent, ablation rates, snow disappearance timing, and
116 sublimation) that are important to cold region hydrology. We select a single model structure and
117 set of parameters to clarify the impact of forcing uncertainty on model outputs. Specifically, we
118 use the physically based Utah Energy Balance (UEB) snow model (Mahat and Tarboton, 2012;
119 Tarboton and Luce, 1996) because it is computationally efficient. The presented framework
120 could be extended to other models.

121

122 **2. Study sites and data**

123 We selected four seasonally snow covered study sites (Table 1) in distinct snow climates (Sturm
124 et al., 1995; Trujillo and Molotch, 2014). The sites included (1) the tundra Innvait Creek (IC,
125 930 m) site (Euskirchen et al., 2012; Kane et al., 1991; Sturm and Wagner, 2010), located north
126 of the Brooks Range in Alaska, USA, (2) the maritime Col de Porte (CDP, 1330 m) site (Morin
127 et al., 2012) in the Chartreuse Range in the Rhône-Alpes of France, (3) the intermountain
128 Reynolds Mountain East (RME, 2060 m) sheltered site (Reba et al., 2011) in the Owyhee Range
129 in Idaho, USA, and (4) the continental Swamp Angel Study Plot (SASP, 3370 m) site (Landry et
130 al., 2014) in the San Juan Mountains of Colorado, USA. We selected these sites because of the
131 quality and completeness of the forcing data, and because they spanned contrasting climates
132 (Table 1), allowing us to check for potential climate-dependencies in sensitivity to forcing errors.
133 Generalization of the results with climate was not possible due to the low sample size of sites.

134

135 The sites had high-quality observations of model forcings at hourly time steps. Serially complete
136 published datasets are available at CDP, RME, and SASP (see citations above). At IC, data were
137 available from multiple co-located stations (Bret-Harte et al., 2010a, 2010b, 2011a, 2011b,
138 2011c; Griffin et al., 2010; Sturm and Wagner, 2010). These data were quality controlled, and
139 gaps in the data were filled as described in Raleigh (2013).

140

141 We considered only one year for analysis at each site (Table 1) due to the high computational
142 costs of the experiment. Measured evaluation data (e.g., snow water equivalent, SWE) at daily
143 resolution were used only for qualitative assessment of model output. SWE was observed at
144 snow pillows at IC and RME. At CDP, a cosmic ray detector collected SWE data. At SASP,
145 acoustic snow depth data were converted to daily SWE using density inferred from nearby
146 SNOw TELemetry (SNOTEL) (Serreze et al., 1999) sites and local snow pit measurements
147 (Raleigh, 2013).

148

149 We adjusted the available precipitation data at each site with a multiplicative factor to correct for
150 potential undercatch errors (e.g., Goodison et al., 1998; Rasmussen et al., 2012; Yang et al.,
151 2000) and to ensure the base model simulation with all observed forcings reasonably represented
152 observed SWE before conducting the sensitivity analysis. Several studies have demonstrated the
153 necessity of precipitation adjustments for realistic SWE simulations, even at well-instrumented
154 sites (e.g., Hiemstra et al., 2006; Reba et al., 2011; Schmucki et al., 2014). Precipitation
155 adjustments were most necessary at IC, where windy conditions preclude effective
156 measurements (Yang et al., 2000). In contrast, only modest adjustments were necessary at the
157 other three sites because they were located in sheltered clearings and because the data already
158 had some corrections applied in the published data. We considered adjustment multipliers
159 ranging from 0.5 to 2.5 (increments of 0.05) and selected the multiplier that yielded the lowest
160 root mean squared error between observed and modeled SWE. Precipitation multipliers were 1.6
161 at IC and 1.15 at SASP, and 0.9 at CDP and RME. The undercatch errors at IC were consistent
162 with the 61-68% undercatch errors found by Yang et al. (2000) for Wyoming-type gauges in
163 wind-blown regions.

164

165 The initial discrepancies between modeled and observed SWE (prior to applying the above
166 precipitation multipliers) may have resulted from deficiencies in the measured forcings, model
167 parameters, model structure, and measured verification data, and justification of our decision to
168 apply precipitation multipliers was warranted. Manual observations of SWE (e.g., snow surveys,
169 snow pits) generally supported the automatically collected SWE observations (no figures
170 shown), and thus differences between observed and modeled SWE did not likely stem from
171 issues in the verification data. Sites where we decreased the precipitation data (CDP and RME)
172 were also the warmer sites and experienced more mixed rain-snow events in the winter. Hence,
173 we considered multiple hypotheses to explain the SWE differences at these sites: (1) the choice
174 of rain-snow parameterization, (2) the choice of parameters (e.g., threshold temperatures) for the
175 rain-snow parameterization, and (3) the quality of the forcing data (e.g., precipitation). For these
176 warmer sites, an exploratory analysis revealed that either (1) or (3) could explain the SWE
177 differences, but auxiliary data (e.g., precipitation phase data) were not available to discriminate
178 these hypotheses. Choosing a different rain-snow parameterization might minimize the SWE
179 differences at the warmer sites but would not rectify the SWE differences at the colder sites (IC

180 and SASP) where most winter precipitation falls as snow. Therefore, the most straightforward
181 and consistent approach was to adjust the precipitation data and to leave the native UEB
182 parameterizations intact. It was beyond the scope of this study to optimize model parameters and
183 unravel the relative contributions of uncertainty for factors other than the meteorological
184 forcings. Nevertheless, we suggest these precipitation adjustments minimally affected the
185 sensitivity analysis, as we did not quantitatively compare the model outputs to the observed
186 response variables (e.g., SWE).

187

188 3. Methods

189 3.1. Model and output metrics

190 The Utah Energy Balance (UEB) is a physically based, one-dimensional snow model (Mahat and
191 Tarboton, 2012; Tarboton and Luce, 1996; You et al., 2013). UEB represents processes such as
192 snow accumulation, snowmelt, albedo decay, surface temperature variation, liquid water
193 retention and refreezing, and sublimation. Due to the one-dimensional structure of the model,
194 UEB does not account for lateral mass transfer of snow (e.g., wind-induced snow drifting), and
195 therefore these processes must be represented in other model components (e.g., precipitation
196 uncertainty, see Sec. 3.2.3). UEB has a single bulk snow layer and an infinitesimally thin
197 surface layer for energy balance computations at the snow-atmosphere interface. UEB tracks
198 state variables for snowpack energy content, SWE, and a dimensionless snow surface age (for
199 albedo computations). We ran UEB at hourly time steps with six forcings: air temperature (T_{air}),
200 precipitation (P), wind speed (U), relative humidity (RH), incoming shortwave radiation (Q_{si}),
201 and incoming longwave radiation (Q_{li}). We used fixed parameters across all scenarios (Table 2).
202 We initialized UEB during the snow-free period; thus, model spin-up was unnecessary.

203

204 With each UEB simulation, we calculated four summary output metrics: (1) peak (i.e.,
205 maximum) SWE, (2) mean ablation rate, (3) snow disappearance date, and (4) total annual snow
206 sublimation. The first three metrics are important for the timing and magnitude of water
207 availability and identification of snowpack regime (Trujillo and Molotch, 2014), while the fourth
208 impacts the partitioning of annual P into runoff and evapotranspiration. We calculated the snow

209 disappearance date as the first date when 90% of peak SWE had ablated, similar to other studies
210 that use a minimum SWE threshold for defining snow disappearance (e.g., Schmucki et al.,
211 2014). The mean ablation rate was calculated in the period between peak SWE and snow
212 disappearance, and was taken as the absolute value of the mean of all SWE decreases.

213

214 **3.2. Forcing error scenarios**

215 To test how error characteristics in forcings affect model outputs, we examined five scenarios
216 (Fig. 1 and Table 3) with different assumptions regarding error types, distributions, and
217 magnitudes (i.e., error ranges). In the first scenario, only bias (normally distributed for additive
218 errors or lognormally distributed for multiplicative precipitation errors) was introduced into all
219 forcings at a level of high uncertainty (based on values observed in the field, see Sec. 3.2.3
220 below). This scenario was named “NB,” where N denotes normal (or lognormal) error
221 distributions and B denotes bias only. The remaining scenarios were identical to NB except one
222 aspect was changed: scenario NB+RE considered both bias and random errors (RE) in all
223 forcings, scenario UB considered uniformly distributed biases in all forcings, scenario NB_gauge
224 considered precipitation error magnitudes associated with gauge undercatch, and scenario
225 NB_lab considered error magnitudes for all forcings at minimal values (i.e., specified instrument
226 accuracy as found in a laboratory). Constructed in this way (Fig. 1), we could test model
227 sensitivity to (1) bias vs. random errors by comparing NB and NB+RE, (2) error distributions by
228 comparing NB and UB, and (3) error magnitudes by comparing NB (high forcing uncertainty) to
229 both NB_gauge (moderate uncertainty in precipitation but high uncertainty for all other forcings)
230 and NB_lab (low forcing uncertainty).

231

232 **3.2.1. Error types**

233 Forcing data inevitably have some (unknown) combination of bias and random errors. However,
234 hydrologic sensitivity analyses have tended to focus more on bias with little or no attention to
235 random errors (Raleigh and Lundquist, 2012), whereas data assimilation methods often focus on
236 random errors but assume bias does not exist (e.g., Dee, 2005). Rarely is there any consideration
237 of interactions between these error types. As a recent example, Lapo et al. (2015) tested biases

238 and random errors in Q_{si} and Q_{li} forcings, finding that biases generally introduced more variance
239 in modeled SWE than random errors. Their experiment considered biases and random errors
240 separately (i.e., no error interactions allowed), and examined only a subset of the required
241 forcings (i.e., radiation). Here, we examined co-existing biases in all forcings in NB, UB,
242 NB_gauge, and NB_lab, and co-existing biases and random errors in all forcings in NB+RE.

243

244 Table 3 shows the assignment of error types for the five scenarios. We relied on studies that
245 assess errors in measurements or estimated forcings to identify typical characteristics of biases
246 and random errors. Published bias values were more straightforward to interpret than random
247 errors because common metrics, such as root mean squared error (RMSE) and mean absolute
248 error (MAE), encapsulate both systematic and random errors. Hence, when defining random
249 errors, published RMSE and MAE served as qualitative guidelines.

250

251 **3.2.2. Error distributions**

252 In their recent review of global sensitivity analysis applications in hydrological modeling, Song
253 et al. (2015) identified the selection of probability distributions (this section) and ranges (Sec.
254 3.2.3) as among the most important considerations. While it is common practice in sensitivity
255 analysis to assume a uniform distribution when sampling model parameters (e.g., Campolongo et
256 al., 2011; Rosero et al., 2010), this may fail to represent the real distribution of errors in
257 meteorological forcing data, as the uniform distribution implies that extreme and small biases are
258 equally probable. It is more likely that real error distributions more closely resemble non-
259 uniform distributions, with higher probability of smaller biases and lower probability of more
260 extreme biases (e.g., normal distributions). Investigators in other fields (e.g., Foscarini et al.,
261 2010; Touhami et al., 2013) have tested how distribution assumptions (uniform vs. normal)
262 change their computed measures of model sensitivity. These studies broadly suggest that the
263 grouping of most important factors may be similar under different distribution assumptions,
264 particularly in cases when interactions are minimal, but the relative ranking of factors within
265 those groups may vary depending on the distribution. Here we test how the assumed probability
266 distribution influences the sensitivity of a snow model to forcing errors.

267

268 We designed the UB scenario with the naive hypothesis that the probability distribution of biases
269 was uniform for all six meteorological variables. In contrast, error distributions (Table 3) were
270 assumed non-uniform (described below) in scenarios NB, NB+RE, NB_gauge, and NB_lab.
271 Unfortunately, error distributions are reported less frequently than error statistics (e.g., bias,
272 RMSE) in the literature. We assumed that T_{air} and RH errors follow normal distributions
273 (Mardikis et al., 2005; Phillips and Marks, 1996), as do Q_{si} and Q_{li} errors. Conflicting reports
274 over the distribution of U indicated that errors may be approximated with a normal (Phillips and
275 Marks, 1996), a lognormal (Mardikis et al., 2005), or a Weibull distribution (Jiménez et al.,
276 2011). For simplicity, we assumed that U errors were normally distributed. Finally, we assumed
277 P errors followed a lognormal distribution to account for snow redistribution due to wind
278 drift/scour (Liston, 2004) or to account for precipitation gauge undercatch (Durand and Margulis,
279 2007). Error distributions were truncated in cases when the introduced errors violated physical
280 limits (e.g., negative U ; see Sec. 3.3.5).

281

282 3.2.3. Error magnitudes

283 We considered three magnitudes of forcing uncertainty (Table 3): levels of uncertainty found (1)
284 in the field for all forcings (i.e., NB), (2) in the field for all forcings except precipitation (which
285 has uncertainty due to precipitation gauge undercatch, i.e., NB_gauge), and (3) in a controlled
286 laboratory setting (i.e., NB_lab). These cases were considered because they sampled realistic
287 errors (NB and NB_gauge) and minimum errors (NB_lab). We expected that the error ranges
288 exerted a major control on model uncertainty and sensitivity, as demonstrated in several prior
289 sensitivity analyses (see review of Song et al., 2015).

290

291 Consideration of error magnitudes was achieved in each scenario by assigning a range to each
292 error probability distribution (see Sec. 3.2.2 and Table 3). While non-uniform distributions (e.g.,
293 normal) are typically described by measures other than the range (e.g., mean and variance), we
294 scaled these distributions (see Sec. 3.3.5 for details) such that they were bounded within a
295 specified range. This convention was necessary to ensure that differences between scenarios NB

296 and UB were due solely to the shape of the error probability distributions, and not due to
297 differences in both distribution shape and the domain. Additionally, this followed the typical
298 practice of sensitivity analysis where the range specifies the domain of the distribution.

299

300 We considered field uncertainties in all forcings in NB, NB+RE, and UB, and in all forcings
301 except precipitation in NB_gauge. Field uncertainties depend on the source of forcing data and
302 on local conditions (e.g., Flerchinger et al., 2009; Lundquist et al., 2015). To generalize the
303 analysis, we chose error ranges for the field uncertainty that enveloped the reported uncertainty
304 of different methods for acquiring forcing data. T_{air} error ranges spanned errors in measurements
305 (Huwald et al., 2009) and commonly used models, such as lapse rates and statistical methods,
306 (Bolstad et al., 1998; Chuanyan et al., 2005; Fridley, 2009; Hasenauer et al., 2003; Phillips and
307 Marks, 1996). U error ranges spanned errors in topographic drift models (Liston and Elder,
308 2006; Winstral et al., 2009) and numerical weather prediction (NWP) models (Cheng and
309 Georgakakos, 2011). RH error ranges spanned errors in observations (Déry and Stieglitz, 2002)
310 and empirical methods (e.g., Bohn et al., 2013; Feld et al., 2013). Q_{si} error ranges spanned errors
311 in empirical methods (Bohn et al., 2013), radiative transfer models (Jing and Cess, 1998),
312 satellite-derived products (Jepsen et al., 2012), and NWP models (Niemelä et al., 2001b). Q_{li}
313 error ranges spanned errors in empirical methods (Bohn et al., 2013; Flerchinger et al., 2009;
314 Herrero and Polo, 2012) and NWP models (Niemelä et al., 2001a).

315

316 P error ranges spanned both undercatch (e.g., Rasmussen et al., 2012) and wind drift/scour errors
317 in NB, NB+RE, and UB, but only undercatch errors in NB_gauge. We assumed that P biases
318 due to gauge undercatch in NB_gauge ranged from -10% to +10% because Meyer et al. (2012)
319 found 95% of SNOTEL sites (often in forest clearings) had observations of accumulated P
320 within 20% of peak SWE. Results of NB, NB+RE, and UB were thus most relevant to areas
321 with prominent snow redistribution (e.g., alpine zone), whereas NB_gauge results were more
322 relevant to areas with minimal wind drift errors. It could be argued that uncertainty due to snow
323 drift processes is a structural issue and not a source of forcing error; however, this distinction
324 depends strongly on what type of model is considered. This process is clearly a structural
325 component for snow models with explicit (e.g., three dimensional models with dynamic wind

326 transport, Lehning et al., 2006) or implicit (one dimensional models with probabilistic subgrid
327 snow variability routines, e.g., Clark et al., 2011a) treatment of snow redistribution. However,
328 when a one dimensional snow model is applied at length scales shorter than drift process length
329 scales (as assumed here with UEB), then it is not possible to account for snow drift in a structural
330 sense. Therefore, we treat drifting snow as a form of precipitation error in NB, NB+RE, and UB.
331 Because UEB lacks dynamic wind redistribution, accumulation uncertainty was not linked to U
332 errors but instead to P errors (e.g., drift factor, Luce et al., 1998).

333

334 In contrast, scenario NB_lab assumed laboratory levels of uncertainty (i.e., measurement
335 accuracy) for each forcing. Skiles et al. (2012) considered a similar scenario in their sensitivity
336 analysis of the SNOBAL model (Marks and Dozier, 1992; Marks et al., 1992) to instrument
337 accuracy at SASP, finding a 5 day range in uncertainty in modeled snow disappearance, with
338 longwave uncertainty having the greatest impact. An emerging sensitivity analysis (Sauter and
339 Obleitner, 2015) with the CROCUS model (Brun et al., 1992) applied on the Kongsvegen
340 Glacier (Svalbard) indicates that longwave measurement uncertainty has an approximately
341 comparable effect on modeled snow depth as $\pm 25\%$ precipitation uncertainty, but is the most
342 dominant influence on the modeled energy balance and turbulent heat flux (relative to the
343 measurement uncertainty of other forcings). Here we build on these efforts to examine how
344 instrument accuracy impacts modeled snow variables in a variety of seasonal snow climates. In
345 general, laboratory uncertainty levels vary with the type and quality of sensors, as well as related
346 accessories (e.g., radiation shield for the temperature sensor), which we did not explicitly
347 consider. Because the actual sensors available varied between sites (Table 1) and we needed
348 consistent errors across sites within scenario NB_lab, we assumed that the manufacturers'
349 specified accuracy of meteorological sensors at a typical SNOTEL site were representative of
350 minimum uncertainties in forcings because of the widespread use of SNOTEL data in snow
351 studies. While we used the specified accuracy for idealized P measurements in NB_lab, we note
352 that the instrument uncertainty of $\pm 3\%$ was likely unrepresentative of errors likely to be
353 encountered. For example, corrections applied to the P data (see Sec. 2) exceeded this
354 uncertainty by factors of 3 to 20.

355

3.3. Sensitivity analysis

Numerous approaches that explore uncertainty in numerical models have been developed in the literature of statistics (Christopher Frey and Patil, 2002), environmental modeling (Matott et al., 2009), and optimization/calibration of hydrology and earth systems models (Beven and Binley, 1992; Duan et al., 1992; Kavetski et al., 2002, 2006a, 2006b; Kuczera et al., 2010; Razavi and Gupta, 2015; Song et al., 2015; Vrugt et al., 2008a, 2008b). Among these, global sensitivity analysis is an elegant platform for testing the impact of input uncertainty on model outputs and for ranking the relative importance of inputs while considering co-existing sources of uncertainty. Global methods are ideal for non-linear models (e.g., snow models). The Sobol' (1990, hereafter Sobol') method is a robust global method based on the decomposition of variance (see below). We investigate Sobol', as it is often the baseline for testing sensitivity analysis methods (Herman et al., 2013; Li et al., 2013; Rakovec et al., 2014; Tang et al., 2007).

3.3.1. Overview: model conceptualization and sensitivity

One can visualize any hydrology or snow model (e.g., UEB) as:

$$\mathbf{Y} = M(\mathbf{F}, \boldsymbol{\theta}) \quad (1)$$

where \mathbf{Y} is a matrix of model outputs (e.g., SWE), $M(\)$ is the model operator, \mathbf{F} is a matrix of forcings (e.g., T_{air} , P , U , etc.), and $\boldsymbol{\theta}$ is an array of model parameters (e.g., Table 2). The goal of sensitivity analysis is to determine which input factors (\mathbf{F} and $\boldsymbol{\theta}$) are most important to specific outputs (\mathbf{Y}) (Matott et al., 2009). Sensitivity analyses tend to focus more on the model parameter array ($\boldsymbol{\theta}$) than on the forcing matrix (Foglia et al., 2009; Herman et al., 2013; Li et al., 2013; Nossent et al., 2011; Rakovec et al., 2014; Rosero et al., 2010; Rosolem et al., 2012; Tang et al., 2007; van Werkhoven et al., 2008). Here, we extend the sensitivity analysis framework to forcing uncertainty by creating k new parameters ($\phi_1, \phi_2, \dots, \phi_k$) that specify forcing uncertainty characteristics (Vrugt et al., 2008b) and reformulate equation 1 as:

$$\mathbf{Y} = M(\mathbf{F}, \boldsymbol{\theta}, \boldsymbol{\phi}) \quad (2)$$

By fixing the original model parameters (Table 2), we focus solely on the influence of forcing errors on model output (\mathbf{Y}). Note it is possible to consider uncertainty in both forcings and parameters in this framework.

385

386 **3.3.2. Sobol' sensitivity analysis**

387 Sobol' sensitivity analysis uses variance decomposition to attribute output variance to input
 388 variance. First-order and higher-order sensitivities can be resolved; here, only the total-order
 389 sensitivities were examined (see below) for clarity and because the resulting first-order
 390 sensitivity indices were typically comparable to the total-order sensitivity indices (e.g., 83% of
 391 all cases had total-order and first-order indices within 10% of each other), suggesting minimal
 392 error interactions. The Sobol' method is advantageous in that it is model independent, can
 393 handle non-linear systems, and is among the most robust sensitivity methods (Saltelli and
 394 Annoni, 2010; Saltelli, 1999). The primary limitation of Sobol' is that it is computationally
 395 intensive, requiring a large number of samples to account for variance across the full parameter
 396 space. A key assumption to the Sobol' approach is that the factors are independent; hence, our
 397 analysis does not consider cases of correlated errors (e.g., a positive measurement bias in T_{air} that
 398 causes a negative RH bias). Below, we provide a brief summary of the Sobol' sensitivity
 399 analysis methodology but note that further details can be found in Saltelli et al. (2010).

400

401 **3.3.3. Sensitivity indices and sampling**

402 Within the Sobol' global sensitivity analysis framework, the total-order sensitivity index (S_{Ti})
 403 describes the variance in model outputs (Y) due to a specific forcing error (ϕ_i), including both
 404 unique (i.e., first-order) effects and all interactions with all other parameters:

$$405 \quad S_{Ti} = \frac{E[V(Y | \phi_{\sim i})]}{V(Y)} = 1 - \frac{V[E(Y | \phi_{\sim i})]}{V(Y)} \quad (3)$$

406 where E is the expectation (i.e., average) operator, V is the variance operator, and $\phi_{\sim i}$ signifies all
 407 parameters except ϕ_i . The latter expression defines S_{Ti} as the variance remaining in Y after
 408 accounting for variance due to all other parameters ($\phi_{\sim i}$). S_{Ti} values have a range of [0, 1].

409 Interpretation of S_{Ti} values was straightforward because they explicitly quantified the variance
 410 introduced to model output by each parameter (i.e., forcing errors). As an example, an S_{Ti} value
 411 of 0.7 for bias parameter ϕ_i on output Y_j indicates 70% of the output variance was due to bias in
 412 forcing i (including unique effects and interactions).

413

414 A number of numerical methods are available for evaluating sensitivity indices, and most adopt a
 415 Monte-Carlo approach (Saltelli et al., 2010). Evaluation of Eq. (3) requires two sampling
 416 matrices, which we refer to as matrices \mathbf{A} and \mathbf{B} (Fig. 2a). To construct \mathbf{A} and \mathbf{B} , we first
 417 specified the number of samples (N) in the parameter space and the number of parameters (k),
 418 depending on the error scenario (Table 3). Selecting sampling points for these two matrices was
 419 achieved using the quasi-random Sobol' sequence (Saltelli and Annoni, 2010). The sequence
 420 can be approximated as a uniform distribution in the range $[0, 1]$. Figure 2a shows an example
 421 Sobol' sequence in two dimensions. For each scenario and site, we generated a $(N \times 2k)$ Sobol'
 422 sequence matrix with quasi-random numbers in the $[0, 1]$ range, and then divided it in two parts
 423 such that matrices \mathbf{A} and \mathbf{B} were each distinct $(N \times k)$ matrices. Calculation of S_{Ti} required
 424 perturbing factors; therefore, a third Sobol' matrix (\mathbf{A}_B) was constructed from \mathbf{A} and \mathbf{B} . In matrix
 425 \mathbf{A}_B , all columns were from \mathbf{A} , except the i th column, which was from the i th column of \mathbf{B} ,
 426 resulting in a $(kN \times k)$ matrix (Fig. 2a). Sec. 3.3.5 provides specific examples of this
 427 implementation. From Eq. (3), we compute S_{Ti} as (Jansen, 1999; Saltelli et al., 2010):

$$428 \quad S_{Ti} = \frac{\frac{1}{2N} \sum_{j=1}^N (f(\mathbf{A})_j - f(\mathbf{A}_B^{(i)})_j)^2}{V(Y)} \quad (4)$$

429 where $f(\mathbf{A})$ is the model output evaluated on the \mathbf{A} matrix, $f(\mathbf{A}_B^{(i)})$ is the model output evaluated
 430 on the \mathbf{A}_B matrix where the i th column is from the \mathbf{B} matrix, and i designates the parameter of
 431 interest. Evaluation of S_{Ti} required $N(k+2)$ simulations at each site and scenario.

432

433 **3.3.4. Bootstrapping of sensitivity indices**

434 To test the reliability of S_{Ti} , we used bootstrapping with replacement across the $N(k+2)$ outputs,
 435 similar to Nossent et al. (2011). The mean and 95% confidence interval were calculated using
 436 the Archer et al. (1997) percentile method and 10 000 samples. For all cases, final S_{Ti} values
 437 were close to the mean bootstrapped values (i.e., 99% had a difference less than 0.001 and no
 438 difference was greater than 0.003), suggesting convergence. Thus, we report only the mean and
 439 95% confidence intervals of the bootstrapped S_{Ti} values.

440

441 3.3.5. Workflow and error introduction

442 Figure 2 shows the workflow for creating the Sobol' \mathbf{A} , \mathbf{B} , and \mathbf{A}_B matrices, mapping Sobol'
443 values to errors, applying errors to the original forcing data, executing the model and saving
444 outputs, and calculating S_{Ti} values. The workflow was repeated at all sites and scenarios. Each
445 step is described in more detail below:

446

447 Step 1) Generate an initial ($N \times 2k$) Sobol' matrix (with N and k values for each scenario, Table
448 3), separate into \mathbf{A} and \mathbf{B} , and construct \mathbf{A}_B (Fig. 2a). NB+RE had $k=12$ (six bias and six random
449 error parameters). All other scenarios had $k=6$ (all bias parameters).

450

451 Step 2) In each simulation, map the Sobol' value of each forcing error parameter (ϕ) to the
452 specified error distribution and range (Fig. 2b, Table 3). Here we treat the Sobol' values as
453 quantiles, which allows us to map the Sobol' values to errors via different probability
454 distributions. For a uniform distribution, the quantile value scales linearly between the specified
455 lower and upper error ranges (Fig. 2b). This linear scaling is not possible for normal (or
456 lognormal) distributions (due to differences in distribution shape) and we therefore map the
457 quantile values to normal (or lognormal) distributions scaled within the specified range. We
458 begin by generating a probability distribution of random numbers with specified mean=0 and
459 standard deviation of 1 for the case of a normal distribution, and with specified mean=20 and
460 standard deviation of 0.5 for the case of a lognormal distribution. The random numbers of the
461 distribution are normalized in the [0, 1] range by subtracting the minimum value and dividing by
462 the maximum value, and then quantiles of these normalized values are computed. The final step
463 of the mapping is to multiply the normalized quantile by the specified range of uncertainty and
464 adding the lower bound value. For example, a Q_{si} bias parameter of $\phi=0.75$ (quantile value) in
465 the $[-100 \text{ W m}^{-2}, +100 \text{ W m}^{-2}]$ range would map to a Q_{si} bias of $+50 \text{ W m}^{-2}$ when assuming a
466 uniform probability distribution but only $+14 \text{ W m}^{-2}$ when assuming a normal distribution. For
467 context, a bias parameter of $+50 \text{ W m}^{-2}$ or higher has about a 25% probability of occurring in the
468 uniform distribution but only 2% in the normal distribution.

469

470 Step 3) In each simulation, perturb (i.e., introduce artificial errors) the observed time series of the
 471 i th forcing (F_i) with bias (all scenarios), or both bias and random errors (NB+RE only) (Fig. 2c):

$$472 \quad F'_i = F_i \phi_{B,i} b_i + (F_i + \phi_{B,i})(1 - b_i) + \phi_{RE,i} R c_i \quad (5)$$

473 where F'_i is the perturbed forcing time series, $\phi_{B,i}$ is the bias parameter for forcing i , b_i is a binary
 474 switch indicating multiplicative bias ($b_i=1$) or additive bias ($b_i=0$), $\phi_{RE,i}$ is the random error
 475 parameter for forcing i , R is a time series of randomly distributed noise (normal distribution,
 476 mean=0) scaled in the [-1, 1] range, and c_i is a binary switch indicating whether random errors
 477 are introduced ($c_i=1$ in scenario NB+RE and $c_i=0$ in all other scenarios). For T_{air} , U , RH , Q_{si} , and
 478 Q_{li} , $b_i=0$; for P , $b_i=1$. The decision to treat biases as multiplicative for P but additive for all
 479 other forcings was made based on practical considerations (e.g., multiplicative bias in T_{air} are
 480 difficult to interpret) and on convention of past studies that report forcing errors. However, we
 481 note this is somewhat subjective, as errors in some forcings (e.g. radiation) have been reported in
 482 both conventions. For P , U , and Q_{si} , we restricted random errors to periods with positive values.
 483 We checked F'_i for non-physical values (e.g., negative Q_{si}) and set these to physical limits. This
 484 was most common when perturbing U , RH , and Q_{si} ; negative values of perturbed P only
 485 occurred when random errors were considered (Eq. 5). Due to this resetting of non-physical
 486 errors, the error distribution was truncated (i.e., it was not always possible to impose extreme
 487 errors). Additional tests (not shown) suggested that distribution truncation changed sensitivity
 488 indices minimally (i.e., <5%), and thus we assumed this truncation did not alter the relative
 489 ranking of forcing errors.

490

491 Step 4) Input the $N(k+2)$ perturbed forcing datasets into UEB (Fig. 2d). At each site, NB+RE
 492 required 140 000 simulations, whereas the other four scenarios each required 80 000 simulations,
 493 for a total of 1 840 000 simulations in the analysis. The doubling of k in NB+RE did not result
 494 in twice as many simulations because the number of simulations scaled as $N(k+2)$.

495

496 Step 5) Save the model outputs for each simulation (Fig. 2e). The outputs included daily time
 497 series of SWE, and four summary outputs including peak SWE, mean ablation rate, snow
 498 disappearance date, and total snow sublimation.

499

500 Step 6) Calculate S_{Ti} for each forcing error parameter and model output (Fig. 2f) based on Sect.
501 3.3.3-3.3.4. Prior to calculating S_{Ti} , we screened the model outputs for cases where UEB
502 simulated too little or too much snow (which can occur with perturbed forcings); this was an
503 essential step to ensure meaningful results. Other studies (e.g., Pappenberger et al., 2008) have
504 also applied screening methods to model output prior to calculating sensitivity indices. For a
505 valid simulation, we required a minimum peak SWE of 50 mm, a minimum continuous snow
506 duration of 15 days, and identifiable snow disappearance. We rejected samples that did not meet
507 these criteria to avoid meaningless or undefined metrics (e.g., peak SWE in ephemeral snow or
508 snow disappearance for a simulation that did not melt out). The number of rejected samples
509 varied with site and scenario (Table 4). On average, 94% passed the requirements. All cases had
510 at least 86% satisfactory samples, except in UB at SASP, where only ~34% met the
511 requirements. In this case, the most common reason for rejecting a simulation was that too much
512 snow was simulated, such that it never disappeared by the end of the model run. The rejected
513 runs were characterized by high (positive) precipitation biases and low (negative) biases in T_{air} ,
514 Q_{si} , and Q_{li} . Despite this attrition, S_{Ti} values still converged in all cases.

515

516 4. Results

517 4.1. Propagation of forcing uncertainty to model outputs

518 Figure 3 shows density plots of daily SWE from UEB at the four sites and five forcing error
519 scenarios (Fig. 1, Table 3), while Fig. 4 summarizes the model outputs. As a reminder, NB
520 assumed normal (or lognormal) biases at field level uncertainty. The other scenarios were the
521 same as NB, except NB+RE considered both biases and random errors, UB considered uniform
522 distributions, NB_gauge considered gauge undercatch biases in precipitation, and NB_lab
523 considered lower error magnitudes in all forcings (i.e., laboratory level uncertainty).

524

525 Large uncertainties in SWE were evident, particularly in NB, NB+RE, and UB (Fig 3.a-l). The
526 large range in modeled SWE within these three scenarios often translated to large ranges in mean
527 ablation rates (Fig 4.e-h), snow disappearance dates (Fig 4.i-l) and total sublimation (Fig 4.m-p).

528 In contrast, SWE and output uncertainties in NB_gauge and NB_lab were comparatively small
529 (Fig. 3m-t and Fig. 4). Model output ranges were generally larger in NB_gauge than NB_lab.
530 The envelope of SWE simulations in NB_lab more tightly encompassed observed SWE at all
531 sites, except during early winter at IC (Fig. 3m), which was possibly due to initial *P* data quality
532 and redistribution of snow to the snow pillow site.

533

534 NB and NB+RE generally yielded similar SWE density plots (Fig. 3a-h), but NB+RE yielded a
535 slightly higher frequency of extreme SWE simulations. NB and NB+RE also had very similar
536 (but not equivalent) mean outputs values and ensemble spreads at all sites except IC (Fig. 4).
537 This initial observation suggested that random errors in the forcings had minimal impact on
538 model behavior at CDP, RME, and SASP. NB+RE and NB model outputs were slightly
539 different at IC (particularly for the ablation rates), indicating that random errors had some
540 influence there, and this was possibly due to the low snow accumulation (~200 mm peak SWE
541 observed) at that site and brief snowmelt season (less than 10 days in the observations).

542

543 NB and UB yielded generally very different model outputs (Fig. 3 and Fig. 4). The only
544 difference in these two scenarios was the assumption regarding error distribution (Table 3).
545 Uniformly distributed forcing biases (scenario UB) yielded a relatively uniform ensemble of
546 SWE simulations (Fig. 3i-l), larger mean values of peak SWE and ablation rates, and later snow
547 disappearance, as well as larger uncertainty ranges in all outputs. At some sites, UB also had a
548 higher frequency of simulations where seasonal sublimation was negative (i.e., condensation).

549

550 Contrasting NB and NB_gauge, NB_gauge had a lower uncertainty range in SWE and slightly
551 higher mean peak SWE at all sites (Fig. 3 and Fig. 4). With the exception of RME, the ranges in
552 ablation rates in NB_gauge were at least 50% smaller than in NB (Fig. 4 e-h). Snow
553 disappearance ranges were marginally smaller in NB_gauge relative to NB (Fig. 4i-l). Finally,
554 sublimation ranges were very similar between NB and NB_gauge (Fig. 4m-p).

555

556 Relative to NB, NB_lab had smaller uncertainty ranges in all model outputs (Fig. 3 and Fig. 4),
557 an expected result given the lower magnitudes in forcing errors in NB_lab (Table 3). Likewise,
558 NB_lab SWE simulations were generally less biased than NB, relative to observations (Fig. 3).
559 NB_lab generally had higher mean peak SWE and ablation rates, and later mean snow
560 disappearance timing than NB (Fig 4).

561

562 **4.2. Model sensitivity to forcing error characteristics**

563 Total-order sensitivity indices (S_{Ti}) were calculated for four summary variables of model output
564 (peak SWE, mean ablation rates, snow disappearance dates, and total sublimation) and for daily
565 SWE output at all sites and error scenarios. Examination of the total-order indices with sample
566 size indicated that most indices stabilized after evaluating the model at 3 000 to 5 000 samples
567 (no figures shown). Below we sequentially compare sensitivity indices from different scenarios
568 to scenario NB to test the impact of differences in error characteristics (type, probability
569 distribution, and magnitudes).

570

571 **4.2.1. Impact of error types**

572 We first focus on sensitivity to forcing bias, as this error type was common to scenarios NB and
573 NB+RE. Figure 5 shows the computed total-order sensitivity indices from the two scenarios
574 (with sensitivities to biases and random errors shown separately in NB+RE). Both NB and
575 NB+RE showed that UEB peak SWE was most sensitive to P bias at all sites (Fig.5a-d). In both
576 scenarios, P bias was also the most important factor for ablation rates and snow disappearance at
577 all sites (Fig. 5e-l). For ablation rates in NB, T_{air} bias was the next most important factor (after P
578 bias) at CDP, while biases in Q_{si} and Q_{li} were secondarily important at RME (Fig.5f-g). For
579 ablation rates at IC in NB+RE, most types of errors had some baseline influence (i.e., $S_{Ti} \geq 0.5$) on
580 model sensitivity (Fig. 5e). In both NB and NB+RE, biases in the radiation terms were of
581 secondary importance to snow disappearance timing (Fig. 5i-k). In contrast to the other three
582 model outputs, sublimation in NB and NB+RE was insensitive to P bias and the most important
583 factors varied somewhat between sites and scenarios (Fig. 5m-p). In both scenarios, sublimation
584 was most sensitive to RH bias at IC and U bias at SASP. At CDP and RME, sublimation was

585 most sensitive to RH bias in NB; however, in NB+RE, sublimation was most sensitive to Q_{li} bias
586 at CDP and to T_{air} bias at RME (Fig. 5n-o). In both scenarios, biases in T_{air} , Q_{si} , or Q_{li} were
587 generally of secondary importance for sublimation.

588

589 We hypothesized that the snow model outputs would have higher sensitivity to biases than to
590 random errors in the forcings. The results of our analysis generally supported this hypothesis.
591 Across all outputs and sites, S_{Ti} values for random errors were always less than or comparable to
592 the smallest S_{Ti} bias values, and the most important factor was always a bias term (Figure 5).
593 Furthermore, there was typically high correspondence between NB and NB+RE (bias terms
594 only) in terms of identifying the most important forcing error (e.g., P bias in peak SWE and
595 ablation rates at all sites, Fig. 5a-h). The main exceptions were snow disappearance at IC (Fig.
596 5i), and sublimation at CDP and RME (Fig. 5n-o), where the two scenarios identified different
597 errors as the most important factor. However, even in these exceptional cases, the two scenarios
598 yielded similar groupings of more important vs. least important errors. For example, biases in
599 T_{air} and RH were important to sublimation at RME in both scenarios (Fig. 5o), though they
600 distinguished these sensitivities differently (i.e., NB found RH bias was more important whereas
601 NB+RE found T_{air} bias was more important).

602

603 While there was general correspondence between NB and NB+RE (bias terms), sensitivity
604 indices were not identical across cases, due to interactions between biases and random errors in
605 NB+RE. Random errors changed model sensitivity to biases, and the change in sensitivity was
606 more notable (i.e., absolute change exceeding 0.10) for ablation rates and snow disappearance at
607 IC (Fig. 5e,i) and sublimation at all sites (Fig. 5m-p). Random errors amplified model sensitivity
608 to biases in some cases (e.g., U bias in all sublimation scenarios) but diminished model
609 sensitivity to biases in other cases (e.g., RH bias in all sublimation scenarios). Because
610 consideration of second-order sensitivity indices was beyond the scope of the study, we were
611 unable to determine which specific interactions were important in terms of error types, and leave
612 this topic for future work.

613

614 **4.2.2. Impact of probability distribution of errors**

615 We hypothesized that the assumed probability distribution of errors would alter the relative
616 hierarchy of forcing biases. However, the results did not consistently support this hypothesis
617 (Fig. 6). In all cases, scenarios NB and UB identified the same factor as the most important and
618 similar factors as the least important at all sites. Specifically, P bias was most important for peak
619 SWE, ablation rates, and snow disappearance at all sites in both scenarios (Fig. 6a-l). The only
620 exception was in scenario UB at IC, where ablation rates had similar sensitivity to P bias and U
621 bias. In both scenarios, T_{air} bias was the second most important factor for peak SWE and
622 ablation rates at the warmest site, CDP. Both scenarios showed that RH bias was the least
623 important factor to snow disappearance at all four sites (Fig. 6i-l). Finally, both NB and UB
624 showed that P bias was least important for sublimation (in contrast to the other model outputs)
625 and that RH and U biases were among the most sensitive factors for sublimation (Fig. 6m-p).
626 More specifically, sublimation was most sensitive to RH bias at IC, CDP, and RME, and U bias
627 as SASP (Fig. 6m-p).

628

629 For a few specific forcings and outputs, the selected probability distribution played a role in
630 model sensitivity to that type of forcing bias. For example, assumption of a uniform probability
631 distribution (UB) for forcing errors enhanced the sensitivity of sublimation to U and RH biases
632 but reduced sublimation sensitivity to Q_{si} and Q_{li} biases at all sites (Fig. 6m-p). In contrast,
633 assuming a normal distribution (NB) of biases yielded the opposite results. Additionally,
634 modeled ablation rates at IC were notably more sensitive to forcing biases (precipitation
635 excluded) in scenario UB than in NB.

636

637 **4.2.3. Impact of error magnitude**

638 We hypothesized that the relative magnitude of forcing errors would exert a strong control on
639 model sensitivity. Comparing NB to NB_gauge and to NB_lab generally supported this
640 hypothesis (Fig. 7). The contrast in S_{Ti} values between scenarios NB, NB_gauge, and NB_lab
641 implied that the specified ranges of forcing errors was a critical determinant of model sensitivity.

642

643 While P bias was the most important factor at all sites in NB for peak SWE, ablation rates, and
644 snow disappearance, P bias was never the most important factor for these model outputs in
645 NB_gauge, and in many cases was among the least important errors (Fig. 7a-l). In NB_gauge,
646 peak SWE was most sensitive to RH bias at IC, T_{air} bias at CDP and RME, and Q_{li} bias at SASP
647 (Fig. 7a-d). Ablation rates in NB_gauge were most sensitive to T_{air} bias at CDP and to Q_{li} bias at
648 IC, RME, and SASP (Fig. 7e-h). Snow disappearance was also most sensitive to Q_{li} bias at all
649 four sites in NB_gauge (Fig. 7i-l). However, for sublimation at all sites, NB and NB_gauge
650 yielded very similar sensitivities to forcing biases (Fig. 7m-p). Specifically, in both NB and
651 NB_gauge, modeled sublimation was most sensitive to RH bias at IC, CDP, and RME and to U
652 bias at SASP (Fig. 7m-p). The similarity in sublimation sensitivity indices between NB and
653 NB_gauge emerged because these scenarios only differed in terms of P uncertainty (Table 3) and
654 because P bias was not important to modeled sublimation. The contrast between sensitivity
655 indices in these two scenarios and for these four outputs illustrated that model sensitivity may
656 depend on both the magnitudes of uncertainty for specific forcings and on the output of interest.

657

658 Whereas NB_gauge demonstrated that reducing the magnitude of forcing uncertainty in one
659 factor (i.e., precipitation) was sufficient to change which factors were most and least important,
660 NB_lab showed that changing the magnitude of forcing uncertainty in all terms could yield a
661 substantially different pattern of model sensitivity (Fig. 7). As a primary example, scenarios NB
662 and NB_lab did not agree whether P bias or Q_{li} bias was the most important factor for peak
663 SWE, ablation rates, and snow disappearance dates at all four sites (Fig. 7a-l). For sublimation,
664 NB_lab sensitivity indices indicated that Q_{li} bias was most important, whereas RH bias (IC,
665 CDP, and RME) and U bias (SASP) were most important in NB (Fig. 7m-p). Across all sites
666 and outputs in NB_lab, Q_{li} bias was consistently the most important factor (Fig. 7). In one sense,
667 this was surprising, given that the bias magnitudes were lower for Q_{li} than for Q_{si} (Table 3).
668 However, the albedo of snow minimizes the amount of energy transmitted to the snowpack from
669 Q_{si} , thereby rendering Q_{si} errors less important than Q_{li} errors. Additionally, the non-linear
670 nature of the model may enhance the role of Q_{li} through interactions with other factors. The
671 general lack of importance in P bias in NB_lab (main exception was peak SWE at IC, Fig. 7a)
672 was due to the discrepancy between the laboratory specified accuracy for P gauges and typical
673 errors encountered in the field.

674

675 **4.2.4. Relative controls of forcing error characteristics on SWE sensitivity**

676 The above results sequentially compared sensitivity indices from different error scenarios to NB
677 in order to ascertain how different assumptions regarding error types, distributions, and
678 magnitudes translated to changes in model sensitivity. To summarize the relative controls of
679 these three forcing error characteristics on model sensitivity, we calculated daily sensitivity
680 indices of modeled SWE to forcing biases at each site and scenario (Fig. 8). We also examined
681 the correspondence between changes in S_{Ti} values and the timing within the snow season.

682

683 Comparing the broad patterns in the time varying S_{Ti} values across the five scenarios, it was
684 evident that error magnitudes were the greatest determinant in model sensitivity to forcing errors
685 through the snow season (compare Fig. 8a-l with Fig. 8m-t). NB, NB+RE, and UB exhibited
686 similar patterns, with high S_{Ti} in P bias throughout the year and with the other forcing biases
687 yielding low S_{Ti} values in the winter and increasing S_{Ti} values in the spring and early summer for
688 some forcings (Fig. 8a-l). In contrast, NB_gauge and NB_lab (Fig. 8m-t) had lower S_{Ti} values
689 for P bias, and more coherent changes in S_{Ti} values that were more synchronized with the
690 specific part of the snow season.

691

692 After error magnitudes, the next most important determinant to model sensitivity was the
693 probabilistic distribution of forcing errors (compare Fig. 8a-d and Fig. 8i-l). Relative to NB, UB
694 tended to yield lower S_{Ti} values for P bias. UB also had higher S_{Ti} values for biases in T_{air} , Q_{li} ,
695 and Q_{si} as time progressed at IC, CDP, and RME (Fig. 8i-k). Finally, the addition of random
696 errors was least important to model sensitivity, as the evolution of S_{Ti} bias values was very
697 similar between NB and NB+RE at most sites (compare Fig. 8a-d and Fig. 8e-h). Random errors
698 mattered the most to modeled SWE at IC, but random errors only changed S_{Ti} values (on
699 average) by less than 10%.

700

701 **5. Discussion**

702 Here we examined the sensitivity of physically-based snow simulations to forcing error
703 characteristics (i.e., types, probability distributions, and magnitudes) using Sobol' global
704 sensitivity analysis. A key result is that among these three characteristics, the magnitude of
705 biases had the most significant impact on UEB simulations (Figs. 3-4) and on model sensitivity
706 (Figs. 7-8). The assumed probability distribution of biases was important in that it increased the
707 range of model outputs (compare NB and UB in Fig. 4), but surprisingly, this usually translated
708 to only modest changes in model sensitivity to forcing errors (Figs. 6 and 8). Random errors
709 were usually less important than biases. Although random errors changed model sensitivity to
710 biases through error interactions, this effect was only large in specific conditions (e.g., ablation
711 rates at IC, Fig. 5e), and the snow model was never more sensitive to random errors than to
712 biases (Fig. 5). Below we discuss these three error characteristics (in order of importance, as
713 suggested by the results), place forcing errors in the context of structural uncertainty, and
714 identify limitations of the analysis and future research directions.

715

716 **5.1. Ranges of error magnitudes**

717 The results supported our hypothesis that the magnitude of biases strongly influences the relative
718 importance of forcing errors. The three magnitudes of uncertainty considered (NB, NB_gauge,
719 and NB_lab) all resulted in different patterns in model sensitivity to forcing biases, and these
720 patterns also varied with the output of interest (Fig. 7). Modeled peak SWE, ablation rates, and
721 snow disappearance were consistently sensitive to P bias in scenario NB and to Q_{li} bias in
722 scenario NB_lab, but there was less consistency in the dominant forcing errors across these three
723 outputs in scenario NB_gauge. While peak SWE, ablation rates, and snow disappearance dates
724 had similar sensitivities to forcing errors (particularly to P biases), sublimation exhibited notably
725 different sensitivity to forcing errors. P bias was frequently the least important factor for
726 sublimation, in contrast to the other model outputs. Biases in RH , U , and T_{air} were often the
727 major controls on modeled sublimation in NB, NB+RE, UB, and NB_gauge, while Q_{li} bias
728 controlled modeled sublimation in NB_lab. These field results partially agree with the
729 sensitivity analysis of Lapp et al. (2005), who showed the most important forcings for
730 sublimation in the Canadian Rockies were U and Q_{si} . However, they did not consider Q_{li} in their
731 sensitivity analysis and so the experiments are not exactly comparable. These results suggest

732 that no single forcing is important across all modeled variables, and model sensitivity strongly
733 depends on the output of interest.

734

735 The dominant effect of P bias on modeled peak SWE, ablation rates, and snow disappearance in
736 the field scenarios (e.g., NB) confirmed previous reports that P uncertainty is a major control on
737 snowpack dynamics (Durand and Margulis, 2008; He et al., 2011b; Schmucki et al., 2014). It
738 was surprising that P bias was often the most critical forcing error for ablation rates in these
739 scenarios (Fig. 5-6). Prior investigations into the relative importance of forcings to ablation were
740 typically framed for a snowpack at the end of winter, such that P uncertainty was not considered
741 (e.g., Zuzel and Cox, 1975). The results here showed that ablation rates were highly sensitive to
742 P bias and this is likely because it controlled the timing and length of the ablation season.

743 Positive P bias extends the fraction of the ablation season in the warmest summer months when
744 ablation rates and radiative energy approach maximum values, whereas negative P bias truncates
745 the fraction of ablation in the warm season. Trujillo and Molotch (2014) reported a similar result
746 based on SNOTEL observations.

747

748 The contrast between scenarios NB, NB_gauge, and NB_lab highlights that selection of the error
749 ranges is a critical step in sensitivity analysis. However, we recognize that there is some
750 subjectivity in the specification of these ranges. Quantification of errors in forcing estimation
751 methods is best achieved through comparisons with surface observations (e.g., Bohn et al., 2013;
752 Flerchinger et al., 2009), but it remains challenging to specify error ranges with confidence
753 (Song et al., 2015). Key considerations controlling the ranges and impacts of forcing errors
754 include the representativeness of the forcing data (e.g., reanalysis, numerical weather model
755 output, extrapolated surface measurements, etc.) in the study area, the length scale of dominant
756 processes (e.g., snow drifting), and the configuration of the snow model (e.g., spatial scale,
757 complexity). Here we selected ranges in the field scenarios to encompass errors encountered
758 across a variety of possible forcing data sources (Table 3), but ultimately the appropriate ranges
759 must be tailored to the specific application. This supports the need for continual evaluation of
760 forcing datasets across a variety of climates and environmental conditions.

761

762 **5.2. Probability distribution of errors**

763 The results did not universally support our hypothesis that the assumed probability distribution
764 of biases was important to the relative ranking of forcing errors. The relative consistency in the
765 dominant forcing errors between NB and UB may have emerged because the probability
766 distributions of all six forcing biases varied together between these two scenarios (i.e., all forcing
767 biases were uniform in UB and either normal or lognormal in NB). While we did not conduct
768 additional tests, we suspect that changing the probability distribution of just a single forcing error
769 (e.g., T_{air} bias) from normal to uniform would have uniquely enhanced model sensitivity to that
770 particular forcing error (Touhami et al., 2013).

771

772 The similarity of results between scenarios NB and UB conform to findings in previous studies
773 (e.g., Foscarini et al., 2010; Touhami et al., 2013) where uniform and normal distributions
774 identified similar factors as the most important. These previous studies imply that greater
775 differences in sensitivity indices (as a function of distribution) will emerge when factor
776 interactions are more prominent. The case with the strongest error interactions here (i.e.,
777 ablation rates at IC) also yielded the largest differences in sensitivity indices between scenarios
778 NB and UB, which is consistent with the prevailing logic.

779

780 **5.3. Error types**

781 The results were consistent with our hypothesis that the snow model is more sensitive to biases
782 than to random errors in the forcings. While previous investigations supported this idea for
783 shortwave and longwave forcings in physically based snow models (i.e., Lapo et al., 2015), the
784 current study showed that biases are more important than random errors for all commonly
785 required meteorological forcings (and not just irradiances). The model was more sensitive to
786 biases and less sensitive to random errors due to the systematic nature of biases. In contrast, the
787 effect of random errors tended to cancel out when integrating model outputs over long periods.
788 Our selected model outputs were generally a function of several months of mass and energy
789 exchange in the snowpack, thereby ensuring minimization of effects from random errors.
790 Random errors only had a greater impact on ablation rates at IC (Fig. 5e), and this was because

791 the relatively brief snowmelt period presented an opportunity for the random errors to not cancel
792 out. Hence, the model may have greater sensitivity to random errors for other model outputs not
793 considered here that integrate over relatively short time scales (e.g., snowmelt over a single day).

794

795 **5.4. Contextualizing forcing and structural uncertainties**

796 Our central argument at the onset was that forcing uncertainty may be comparable to parametric
797 and structural uncertainty in snow-affected catchments. To support our argument and to place
798 our results in context, we compare our results at CDP in 2005-2006 to Essery et al. (2013), who
799 assessed the impact of structural uncertainty in a suite of local snowpack processes (i.e., snow
800 compaction, fresh snow density, snow albedo evolution, surface heat and moisture fluxes, snow
801 cover fraction, snow hydrology, and thermal conductivity) on SWE simulations from 1701
802 physically based snow models at the same site/year. Figure 9 compares the 95% uncertainty
803 ranges in peak SWE, ablation rates, and snow disappearance in NB, NB_gauge, and NB_lab to
804 the ranges found across the 1701 snow models of Essery et al. (2013). From the comparisons at
805 this site, it is clear that the uncertainty associated with drifting snow (i.e., scenario NB)
806 overwhelms the structural uncertainty in local snowpack processes for all three model outputs.
807 As discussed previously, it could be argued that the uncertainty due to drifting snow is a
808 structural issue (not a forcing issue) and that this does not represent the uncertainty of sheltered
809 areas where drifting snow less important. Hence, NB_gauge may be a better determinant of the
810 level of uncertainty that can be attributed unambiguously to errors in forcing data. In that case,
811 the output uncertainty range due to model forcing is still larger than that due to the structural
812 uncertainty (as considered by Essery et al., 2013) in the cases of peak SWE and snow
813 disappearance but is smaller for ablation rates (Fig. 9). As expected, the case of forcing
814 uncertainty in NB_lab yields the lowest range in model outputs at CDP (Fig. 9), though it is
815 interesting to note that the uncertainty in peak SWE due to structural uncertainty (90 mm) is only
816 marginally larger than that due to the specified instrument accuracy (60 mm). These
817 comparisons illustrate that forcing uncertainty cannot be discounted, and the magnitude of
818 forcing uncertainty is a critical factor in how forcing uncertainty compares to other sources of
819 uncertainty (e.g., structural). This resonates with the recent work of Magnusson et al. (2015)

820 who found that uncertainty in the P forcing was a greater determinant of model performance than
821 structural considerations.

822

823 **5.5. Caveats and future research**

824 Limitations of the analysis are that the impact of forcing error characteristics on model behavior
825 is evaluated through the lens of a single sensitivity analysis method and a single snow model. It
826 is possible that alternative sensitivity analysis methods might yield different results than the
827 Sobol' method, as suggested in previous studies (e.g., Pappenberger et al., 2008). Likewise, we
828 recognize it is possible that different snow models may yield different sensitivities to forcing
829 uncertainty. As one example, both Koivusalo and Heikinheimo (1999) and Lapo et al. (2015)
830 found UEB (Tarboton and Luce, 1996) and the SNTHERM model (Jordan, 1991) exhibited
831 significant differences in radiative and turbulent heat exchange. As another example, the role of
832 U bias on snowpack formation may vary strongly depending on the snow model configuration.
833 Because of the lack of wind transport in UEB, we lumped snow drift uncertainty into P
834 uncertainty via a "drift factor" formulation (Luce et al., 1998) and this could not account for the
835 role of wind in snow drift/scour processes (Mott and Lehning, 2010; Winstral et al., 2013). This
836 convention would be unnecessary for a model that explicitly models this process (e.g., the
837 SNOWPACK model, Lehning et al., 2006), and for this type of model we would expect the role
838 of U bias to be enhanced (relative to UEB) for outputs such as peak SWE and snow
839 disappearance timing. While sensitivity may vary with model selection in these examples, there
840 is also evidence suggesting that similar results may emerge when using different snow models
841 for a similar type of error scenario. Despite using different models, a somewhat different suite of
842 forcing variables, and slightly different error ranges, our NB_lab experiment corroborated
843 independent reports that Q_{li} measurement uncertainty was most important to both modeled snow
844 disappearance (Skiles et al., 2012) and sublimation/latent heat exchange (Sauter and Obleitner,
845 2015). Our analysis demonstrated this result was consistent across four snow climates and this
846 result was apparent in four different model outputs (Fig. 7). The implication here is that more
847 work is needed to better understand how different snow models respond to forcing uncertainty.

848

849 Generalizing the relationship between model sensitivity and site climate is a research topic of
850 high interest. Although we found similarities in model sensitivity to specific forcing errors
851 across sites (e.g., high sensitivity to P bias in peak SWE, ablation rates, and snow disappearance
852 in NB, NB+RE, and UB, Fig. 8a-l), we note that the sites exhibited some differences in
853 sensitivity when P uncertainty was reduced to gauge levels (Fig. 8m-p). Additionally, the sites
854 exhibited differences in the relative importance of secondary forcing errors (Fig. 6-7). There
855 may be interesting linkages between climate and model sensitivity, but we were unable to
856 generalize relationships between site geo-characteristics and sensitivity indices because of the
857 relatively low number of sites represented here (n=4 sites, 1 year each) and the confounding
858 number of differences between sites. A much larger population of snow measurement sites is
859 required in order to test relationships between sensitivity indices and site characteristics, and this
860 is an important avenue of future research. A successful example of relating climate
861 characteristics to sensitivity indices when many study sites and years are available can be found
862 in van Werkhoven et al. (2008).

863

864 While the Sobol' method is often considered the "baseline" method in global sensitivity analysis,
865 we note the limitation is that it comes at a relatively high computation cost (1 840 000
866 simulations across four sites and five error scenarios) and it may be prohibitive for many
867 modeling applications (e.g., for models of higher complexity and dimensionality). For context,
868 the typical time required for a single simulation was 1.4 seconds, resulting in a total
869 computational expense of 720 hours (30 days) across all scenarios. Examination of the
870 convergence rates indicated that most sensitivity indices stabilized after one-third of the
871 simulations completed, and hence the same results could have been found using significantly
872 fewer simulations (no figures shown). Ongoing research is developing new sensitivity analysis
873 methods that compare well to Sobol' but with reduced computational demands (e.g., FAST,
874 Cukier, 1973; method of Morris, 1991; DELSA, Rakovec et al., 2014), and is comparing how
875 different methods classify sensitive factors differently (Pappenberger et al., 2008; Tang et al.,
876 2007). We expect that detailed sensitivity analyses that concurrently consider uncertainty in
877 forcings, parameters, and structure in a hydrologic model will be more feasible in the future with
878 better computing resources and advances in sensitivity analysis methods.

879

880 The question remains: “what can be done about forcing errors in hydrologic modeling?” First,
881 the results suggest model-based hypothesis testing must account for uncertainties in forcing data.
882 The results also highlight the need for continued research in constraining P uncertainty in snow-
883 affected catchments. Progress is being achieved with advanced pathways for quantifying
884 snowfall precipitation, such as NWP models (Rasmussen et al., 2011, 2014) and through
885 systematic intercomparisons of precipitation and snow gauges (e.g., Solid Precipitation
886 Intercomparison Experiment, <http://www.rap.ucar.edu/projects/SPICE/>). However, in a broader
887 sense, the hydrologic community should also consider whether deterministic forcings (i.e., single
888 time series for each forcing) are a reasonable practice for physically-based models, given the
889 large uncertainties in both future (e.g., climate change) and historical data (especially in poorly
890 monitored catchments) and the complexities of hydrologic systems (Gupta et al., 2008). We
891 suggest that probabilistic model forcings (e.g., Clark and Slater, 2006), which have a legacy in
892 data assimilation methods (e.g., precipitation uncertainty, Durand and Margulis, 2007), present
893 one potential path forward where measures of forcing uncertainty can be explicitly included in
894 the forcing datasets. The challenges are (1) to ensure statistical reliability in our understanding
895 of forcing errors and (2) to assess how best to input probabilistic forcings into current model
896 architectures.

897

898 **6. Conclusions**

899 Application of the Sobol’ sensitivity analysis framework across sites in contrasting snow
900 climates reveals that forcing uncertainty can significantly impact model behavior in snow-
901 affected catchments. Model output uncertainty due to forcings can be comparable to or larger
902 than model uncertainty due to model structure. Furthermore, this work demonstrates that
903 sensitivity analysis can be applied to understand the role of specific error characteristics in model
904 behavior. Key considerations in model sensitivity to forcing errors are the magnitudes of forcing
905 errors and the outputs of interest. For the physically-based snow model tested, random errors in
906 forcings are generally less important than biases, and the probability distribution of biases is
907 relatively less important to model sensitivity than the magnitude of biases.

908

909 The analysis shows how forcing uncertainty might be included in a formal sensitivity analysis
910 framework through the introduction of new parameters that specify the characteristics of forcing
911 uncertainty. The framework could be extended to other physically based models and sensitivity
912 analysis methodologies, and could be used to quantify how uncertainties in model forcings and
913 parameters interact. Based on this framework, it would be interesting to assess the interplay
914 between co-existing uncertainties in forcing errors, model parameters, and model structure, and
915 to test how model sensitivity changes relative to all three sources of uncertainty.

916

917 **Acknowledgements**

918 M. Raleigh was supported by a post-doctoral fellowship in the Advanced Study Program at the
919 National Center for Atmospheric Research (NCAR). NCAR is sponsored by the National
920 Science Foundation. J. Lundquist was supported by NSF (EAR-838166 and EAR-1215771).
921 The manuscript was improved thanks to thoughtful comments from F. Pianosi, J. Li, R. Essery,
922 R. Rosolem, A. Winstral, and one anonymous reviewer. Thanks to M. Sturm, G. Shaver, S.
923 Bret-Harte, and E. Euskirchen for assistance with Innavait Creek data, S. Morin for assistance
924 with Col de Porte data, D. Marks for assistance with Reynolds Mountain data, C. Landry for
925 assistance with Swamp Angel data, and E. Gutmann and P. Mendoza for feedback. For Innavait
926 Creek data, we acknowledge U.S. Army Cold Regions Research and Engineering Laboratory, the
927 NSF Arctic Observatory Network (AON) Carbon, Water, and Energy Flux monitoring project
928 and the Marine Biological Laboratory, Woods Hole, and the University of Alaska, Fairbanks.
929 The experiment was improved thanks to conversations with D. Slater.

930

931 **References**

932 Archer, G. E. B., Saltelli, A. and Sobol, I. M.: Sensitivity measures, anova-like Techniques and
933 the use of bootstrap, *J. Stat. Comput. Simul.*, 58(2), 99–120, doi:10.1080/00949659708811825,
934 1997.

935 Di Baldassarre, G. and Montanari, A.: Uncertainty in river discharge observations: a quantitative
936 analysis, *Hydrol. Earth Syst. Sci.*, 13(6), 913–921, doi:10.5194/hess-13-913-2009, 2009.

- 937 Bales, R. C., Molotch, N. P., Painter, T. H., Dettinger, M. D., Rice, R. and Dozier, J.: Mountain
938 hydrology of the western United States, *Water Resour. Res.*, 42, W08432,
939 doi:10.1029/2005WR004387, 2006.
- 940 Barnett, T. P., Pierce, D. W., Hidalgo, H. G., Bonfils, C., Santer, B. D., Das, T., Bala, G., Wood,
941 A. W., Nozawa, T., Mirin, A. A., Cayan, D. R. and Dettinger, M. D.: Human-induced changes in
942 the hydrology of the western United States, *Science (80-.)*, 319(5866), 1080–1083,
943 doi:10.1126/science.1152538, 2008.
- 944 Bastola, S., Murphy, C. and Sweeney, J.: The role of hydrological modelling uncertainties in
945 climate change impact assessments of Irish river catchments, *Adv. Water Resour.*, 34(5), 562–
946 576, doi:10.1016/j.advwatres.2011.01.008, 2011.
- 947 Benke, K. K., Lowell, K. E. and Hamilton, A. J.: Parameter uncertainty, sensitivity analysis and
948 prediction error in a water-balance hydrological model, *Math. Comput. Model.*, 47(11-12),
949 1134–1149, doi:10.1016/j.mcm.2007.05.017, 2008.
- 950 Beven, K. and Binley, A.: The future of distributed models: model calibration and uncertainty
951 prediction, *Hydrol. Process.*, 6(3), 279–298, doi:10.1002/hyp.3360060305, 1992.
- 952 Bohn, T. J., Livneh, B., Oyler, J. W., Running, S. W., Nijssen, B. and Lettenmaier, D. P.: Global
953 evaluation of MTCLIM and related algorithms for forcing of ecological and hydrological
954 models, *Agric. For. Meteorol.*, 176, 38–49, doi:10.1016/j.agrformet.2013.03.003, 2013.
- 955 Bolstad, P. V., Swift, L., Collins, F. and Régnière, J.: Measured and predicted air temperatures at
956 basin to regional scales in the southern Appalachian mountains, *Agric. For. Meteorol.*, 91(3-4),
957 161–176, doi:10.1016/S0168-1923(98)00076-8, 1998.
- 958 Bret-Harte, S., Euskirchen, E., Griffin, K. and Shaver, G.: Eddy Flux Measurements, Tussock
959 Station, Innvait Creek, Alaska - 2011, , Long Term Ecological Research Network,
960 doi:10.6073/pasta/44a62e0c6741b3bd93c0a33e7b677d90, 2011a.
- 961 Bret-Harte, S., Euskirchen, E. and Shaver, G.: Eddy Flux Measurements, Fen Station, Innvait
962 Creek, Alaska - 2011, , Long Term Ecological Research Network,
963 doi:10.6073/pasta/50e9676f29f44a8b6677f05f43268840, 2011b.
- 964 Bret-Harte, S., Euskirchen, E. and Shaver, G.: Eddy Flux Measurements, Ridge Station, Innvait
965 Creek, Alaska - 2011, , Long Term Ecological Research Network,
966 doi:10.6073/pasta/5d603c3628f53f494f08f895875765e8, 2011c.
- 967 Bret-Harte, S., Shaver, G. and Euskirchen, E.: Eddy Flux Measurements, Fen Station, Innvait
968 Creek, Alaska - 2010, , Long Term Ecological Research Network,
969 doi:10.6073/pasta/dde37e89dab096bea795f5b111786c8b, 2010a.

- 970 Bret-Harte, S., Shaver, G. and Euskirchen, E.: Eddy Flux Measurements, Ridge Station, Imnavait
971 Creek, Alaska - 2010, , Long Term Ecological Research Network,
972 doi:10.6073/pasta/fb047eaa2c78d4a3254bba8369e6cee5, 2010b.
- 973 Brun, E., David, P., Sudul, M. and Brunot, G.: A numerical model to simulate snow-cover
974 stratigraphy for operational avalanche forecasting, *J. Glaciol.*, 38(128), 13–22, 1992.
- 975 Burles, K. and Boon, S.: Snowmelt energy balance in a burned forest plot, Crowsnest Pass,
976 Alberta, Canada, *Hydrol. Process.*, doi:10.1002/hyp.8067, 2011.
- 977 Butts, M. B., Payne, J. T., Kristensen, M. and Madsen, H.: An evaluation of the impact of model
978 structure on hydrological modelling uncertainty for streamflow simulation, *J. Hydrol.*, 298(1-4),
979 242–266, doi:10.1016/j.jhydrol.2004.03.042, 2004.
- 980 Campolongo, F., Saltelli, A. and Cariboni, J.: From screening to quantitative sensitivity analysis.
981 A unified approach, *Comput. Phys. Commun.*, 182(4), 978–988, doi:10.1016/j.cpc.2010.12.039,
982 2011.
- 983 Cheng, F.-Y. and Georgakakos, K. P.: Statistical analysis of observed and simulated hourly
984 surface wind in the vicinity of the Panama Canal, *Int. J. Climatol.*, 31(5), 770–782,
985 doi:10.1002/joc.2123, 2011.
- 986 Christopher Frey, H. and Patil, S. R.: Identification and Review of Sensitivity Analysis Methods,
987 *Risk Anal.*, 22(3), 553–578, doi:10.1111/0272-4332.00039, 2002.
- 988 Chuanyan, Z., Zhongren, N. and Guodong, C.: Methods for modelling of temporal and spatial
989 distribution of air temperature at landscape scale in the southern Qilian mountains, China, *Ecol.*
990 *Modell.*, 189(1-2), 209–220, doi:10.1016/j.ecolmodel.2005.03.016, 2005.
- 991 Clark, M. P., Hendrikx, J., Slater, A. G., Kavetski, D., Anderson, B., Cullen, N. J., Kerr, T., Örn
992 Hreinsson, E. and Woods, R. A.: Representing spatial variability of snow water equivalent in
993 hydrologic and land-surface models: A review, *Water Resour. Res.*, 47(7),
994 doi:10.1029/2011WR010745, 2011a.
- 995 Clark, M. P., Kavetski, D. and Fenicia, F.: Pursuing the method of multiple working hypotheses
996 for hydrological modeling, *Water Resour. Res.*, 47(9), 1–16, doi:10.1029/2010WR009827,
997 2011b.
- 998 Clark, M. P., Nijssen, B., Lundquist, J. D., Kavetski, D., Rupp, D. E., Woods, R. A., Freer, J. E.,
999 Gutmann, E. D., Wood, A. W., Brekke, L. D., Arnold, J. R., Gochis, D. J. and Rasmussen, R. M.:
1000 A unified approach for process-based hydrologic modeling: 1. Modeling concept, *Water Resour.*
1001 *Res.*, 51, doi:10.1002/2015WR017198, 2015a.
- 1002 Clark, M. P., Nijssen, B., Lundquist, J. D., Kavetski, D., Rupp, D. E., Woods, R. A., Freer, J. E.,
1003 Gutmann, E. D., Wood, A. W., Gochis, D. J., Rasmussen, R. M., Tarboton, D. G., Mahat, V.,
1004 Flerchinger, G. N. and Marks, D. G.: A unified approach for process-based hydrologic modeling:

- 1005 2. Model implementation and case studies, *Water Resour. Res.*, 51,
1006 doi:10.1002/2015WR017200, 2015b.
- 1007 Clark, M. P. and Slater, A. G.: Probabilistic Quantitative Precipitation Estimation in Complex
1008 Terrain, *J. Hydrometeorol.*, 7(1), 3–22, doi:10.1175/JHM474.1, 2006.
- 1009 Clark, M. P., Slater, A. G., Rupp, D. E., Woods, R. A., Vrugt, J. A., Gupta, H. V., Wagener, T.
1010 and Hay, L. E.: Framework for Understanding Structural Errors (FUSE): A modular framework
1011 to diagnose differences between hydrological models, *Water Resour. Res.*, 44(12),
1012 doi:10.1029/2007WR006735, 2008.
- 1013 Cukier, R. I.: Study of the sensitivity of coupled reaction systems to uncertainties in rate
1014 coefficients. I Theory, *J. Chem. Phys.*, 59(8), 3873, doi:10.1063/1.1680571, 1973.
- 1015 Dadic, R., Mott, R., Lehning, M., Carenzo, M., Anderson, B. and Mackintosh, A.: Sensitivity of
1016 turbulent fluxes to wind speed over snow surfaces in different climatic settings, *Adv. Water*
1017 *Resour.*, 55, 178–189, doi:10.1016/j.advwatres.2012.06.010, 2013.
- 1018 Dee, D. P.: Bias and data assimilation, *Q. J. R. Meteorol. Soc.*, 131(613), 3323–3343,
1019 doi:10.1256/qj.05.137, 2005.
- 1020 Deems, J. S., Painter, T. H., Barsugli, J. J., Belnap, J. and Udall, B.: Combined impacts of
1021 current and future dust deposition and regional warming on Colorado River Basin snow
1022 dynamics and hydrology, *Hydrol. Earth Syst. Sci.*, 17(11), 4401–4413, doi:10.5194/hess-17-
1023 4401-2013, 2013.
- 1024 Déry, S. and Stieglitz, M.: A note on surface humidity measurements in the cold Canadian
1025 environment, *Boundary-Layer Meteorol.*, 102, 491–497, doi:10.1023/A:1013890729982, 2002.
- 1026 Duan, Q., Sorooshian, S. and Gupta, V.: Effective and efficient global optimization for
1027 conceptual rainfall-runoff models, *Water Resour. Res.*, 28(4), 1015–1031,
1028 doi:10.1029/91WR02985, 1992.
- 1029 Durand, M. and Margulis, S. A.: Correcting first-order errors in snow water equivalent estimates
1030 using a multifrequency, multiscale radiometric data assimilation scheme, *J. Geophys. Res.*,
1031 112(D13), 1–15, doi:10.1029/2006JD008067, 2007.
- 1032 Durand, M. and Margulis, S. A.: Effects of uncertainty magnitude and accuracy on assimilation
1033 of multiscale measurements for snowpack characterization, *J. Geophys. Res.*, 113(D2), D02105,
1034 doi:10.1029/2007JD008662, 2008.
- 1035 Elsner, M. M., Gangopadhyay, S., Pruitt, T., Brekke, L. D., Mizukami, N. and Clark, M. P.: How
1036 Does the Choice of Distributed Meteorological Data Affect Hydrologic Model Calibration and
1037 Streamflow Simulations?, *J. Hydrometeorol.*, 15(4), 1384–1403, doi:10.1175/JHM-D-13-083.1,
1038 2014.

- 1039 Essery, R., Morin, S., Lejeune, Y. and B Ménard, C.: A comparison of 1701 snow models using
1040 observations from an alpine site, *Adv. Water Resour.*, 55, 131–148,
1041 doi:10.1016/j.advwatres.2012.07.013, 2013.
- 1042 Euskirchen, E. S., Bret-Harte, M. S., Scott, G. J., Edgar, C. and Shaver, G. R.: Seasonal patterns
1043 of carbon dioxide and water fluxes in three representative tundra ecosystems in northern Alaska,
1044 *Ecosphere*, 3(1), doi:10.1890/ES11-00202.1, 2012.
- 1045 Feld, S. I., Cristea, N. C. and Lundquist, J. D.: Representing atmospheric moisture content along
1046 mountain slopes: Examination using distributed sensors in the Sierra Nevada, California, *Water*
1047 *Resour. Res.*, 49, doi:10.1002/wrcr.20318, 2013.
- 1048 Flerchinger, G. N., Xaio, W., Marks, D., Sauer, T. J. and Yu, Q.: Comparison of algorithms for
1049 incoming atmospheric long-wave radiation, *Water Resour. Res.*, 45(3), 1–13,
1050 doi:10.1029/2008WR007394, 2009.
- 1051 Flint, A. L. and Childs, S. W.: Calculation of solar radiation in mountainous terrain, *Agric. For.*
1052 *Meteorol.*, 40(3), 233–249, doi:10.1016/0168-1923(87)90061-X, 1987.
- 1053 Foglia, L., Hill, M. C., Mehl, S. W. and Burlando, P.: Sensitivity analysis, calibration, and
1054 testing of a distributed hydrological model using error-based weighting and one objective
1055 function, *Water Resour. Res.*, 45(6), doi:10.1029/2008WR007255, 2009.
- 1056 Foscarini, F., Bellocchi, G., Confalonieri, R., Savini, C. and Van den Eede, G.: Sensitivity
1057 analysis in fuzzy systems: Integration of SimLab and DANA, *Environ. Model. Softw.*, 25(10),
1058 1256–1260, doi:10.1016/j.envsoft.2010.03.024, 2010.
- 1059 Fridley, J. D.: Downscaling Climate over Complex Terrain: High Finescale (<1000 m) Spatial
1060 Variation of Near-Ground Temperatures in a Montane Forested Landscape (Great Smoky
1061 Mountains)*, *J. Appl. Meteorol. Climatol.*, 48(5), 1033–1049, doi:10.1175/2008JAMC2084.1,
1062 2009.
- 1063 Georgakakos, K., Seo, D., Gupta, H., Schaake, J. and Butts, M.: Towards the characterization of
1064 streamflow simulation uncertainty through multimodel ensembles, *J. Hydrol.*, 298(1-4), 222–
1065 241, doi:10.1016/j.jhydrol.2004.03.037, 2004.
- 1066 Goodison, B., Louie, P. and Yang, D.: WMO solid precipitation measurement intercomparison:
1067 Final report, in *Instrum. Obs. Methods Rep. 67*, vol. 67, p. 211, World Meteorol. Organ.,
1068 Geneva, Switzerland., 1998.
- 1069 Griffin, K., Bret-Harte, S., Shaver, G. and Euskirchen, E.: Eddy Flux Measurements, Tussock
1070 Station, Innvait Creek, Alaska - 2010, , Long Term Ecological Research Network,
1071 doi:10.6073/pasta/7bba82256e0f5d9ec3d2bc9c25ab9bcf, 2010.

- 1072 Guan, B., Molotch, N. P., Waliser, D. E., Jepsen, S. M., Painter, T. H. and Dozier, J.: Snow
1073 water equivalent in the Sierra Nevada: Blending snow sensor observations with snowmelt model
1074 simulations, *Water Resour. Res.*, 49(8), 5029–5046, doi:10.1002/wrcr.20387, 2013.
- 1075 Guan, H., Wilson, J. L. and Makhnin, O.: Geostatistical Mapping of Mountain Precipitation
1076 Incorporating Autosearched Effects of Terrain and Climatic Characteristics, *J. Hydrometeorol.*,
1077 6(6), 1018–1031, doi:10.1175/JHM448.1, 2005.
- 1078 Gupta, H. V., Wagener, T. and Liu, Y.: Reconciling theory with observations: elements of a
1079 diagnostic approach to model evaluation, *Hydrol. Process.*, 22, 3802–3813,
1080 doi:10.1002/hyp.6989, 2008.
- 1081 Hasenauer, H., Merganicova, K., Petritsch, R., Pietsch, S. A. and Thornton, P. E.: Validating
1082 daily climate interpolations over complex terrain in Austria, *Agric. For. Meteorol.*, 119, 87–107,
1083 doi:10.1016/S0168-1923(03)00114-X, 2003.
- 1084 He, M., Hogue, T. S., Franz, K. J., Margulis, S. A. and Vrugt, J. A.: Characterizing parameter
1085 sensitivity and uncertainty for a snow model across hydroclimatic regimes, *Adv. Water Resour.*,
1086 34(1), 114–127, doi:10.1016/j.advwatres.2010.10.002, 2011a.
- 1087 He, M., Hogue, T. S., Franz, K. J., Margulis, S. A. and Vrugt, J. A.: Corruption of parameter
1088 behavior and regionalization by model and forcing data errors: A Bayesian example using the
1089 SNOW17 model, *Water Resour. Res.*, 47(7), 1–17, doi:10.1029/2010WR009753, 2011b.
- 1090 Herman, J. D., Kollat, J. B., Reed, P. M. and Wagener, T.: Technical Note: Method of Morris
1091 effectively reduces the computational demands of global sensitivity analysis for distributed
1092 watershed models, *Hydrol. Earth Syst. Sci.*, 17(7), 2893–2903, doi:10.5194/hess-17-2893-2013,
1093 2013.
- 1094 Herrero, J. and Polo, M. J.: Parameterization of atmospheric longwave emissivity in a
1095 mountainous site for all sky conditions, *Hydrol. Earth Syst. Sci.*, 16(9), 3139–3147,
1096 doi:10.5194/hess-16-3139-2012, 2012.
- 1097 Hiemstra, C. A., Liston, G. E. and Reiners, W. A.: Observing, modelling, and validating snow
1098 redistribution by wind in a Wyoming upper treeline landscape, *Ecol. Modell.*, 197(1-2), 35–51,
1099 doi:10.1016/j.ecolmodel.2006.03.005, 2006.
- 1100 Hutchinson, M. F., McKenney, D. W., Lawrence, K., Pedlar, J. H., Hopkinson, R. F., Milewska,
1101 E. and Papadopol, P.: Development and Testing of Canada-Wide Interpolated Spatial Models of
1102 Daily Minimum–Maximum Temperature and Precipitation for 1961–2003, *J. Appl. Meteorol.*
1103 *Climatol.*, 48(4), 725–741, doi:10.1175/2008JAMC1979.1, 2009.
- 1104 Huwald, H., Higgins, C. W., Boldi, M.-O., Bou-Zeid, E., Lehning, M. and Parlange, M. B.:
1105 Albedo effect on radiative errors in air temperature measurements, *Water Resour. Res.*, 45(8), 1–
1106 13, doi:10.1029/2008WR007600, 2009.

- 1107 Jackson, C., Xia, Y., Sen, M. K. and Stoffa, P. L.: Optimal parameter and uncertainty estimation
1108 of a land surface model: A case study using data from Cabauw, Netherlands, *J. Geophys. Res.*,
1109 108(D18), 4583, doi:10.1029/2002JD002991, 2003.
- 1110 Jansen, M. J. W.: Analysis of variance designs for model output, *Comput. Phys. Commun.*,
1111 117(1-2), 35–43, doi:10.1016/S0010-4655(98)00154-4, 1999.
- 1112 Jepsen, S. M., Molotch, N. P., Williams, M. W., Rittger, K. E. and Sickman, J. O.: Interannual
1113 variability of snowmelt in the Sierra Nevada and Rocky Mountains, United States: Examples
1114 from two alpine watersheds, *Water Resour. Res.*, 48(2), 1–15, doi:10.1029/2011WR011006,
1115 2012.
- 1116 Jiménez, P. A., Dudhia, J. and Navarro, J.: On the surface wind speed probability density
1117 function over complex terrain, *Geophys. Res. Lett.*, 38(22), doi:10.1029/2011GL049669, 2011.
- 1118 Jing, X. and Cess, R. D.: Comparison of atmospheric clear-sky shortwave radiation models to
1119 collocated satellite and surface measurements in Canada, *J. Geophys. Res.*, 103(D22), 28817,
1120 doi:10.1029/1998JD200012, 1998.
- 1121 Jordan, R.: A One-Dimensional Temperature Model for a Snow Cover: Technical
1122 Documentation for SNTHERM.89, p. 58, Special Report 91-16, US Army CRREL, Hanover,
1123 NH, USA., 1991.
- 1124 Kane, D. L., Hinzman, L. D., Benson, C. S. and Liston, G. E.: Snow hydrology of a headwater
1125 Arctic basin: 1. Physical measurements and process studies, *Water Resour. Res.*, 27(6), 1099–
1126 1109, doi:10.1029/91WR00262, 1991.
- 1127 Kavetski, D., Franks, S. W. and Kuczera, G.: Confronting input uncertainty in environmental
1128 modelling, in *Calibration of Watershed Models*, edited by Q. Duan, H. V. Gupta, S. Sorooshian,
1129 A. N. Rousseau, and R. Turcotte, pp. 49–68, American Geophysical Union, Washington, D.C.,
1130 2002.
- 1131 Kavetski, D., Kuczera, G. and Franks, S. W.: Bayesian analysis of input uncertainty in
1132 hydrological modeling: 1. Theory, *Water Resour. Res.*, 42(3), W03407,
1133 doi:10.1029/2005WR004368, 2006a.
- 1134 Kavetski, D., Kuczera, G. and Franks, S. W.: Bayesian analysis of input uncertainty in
1135 hydrological modeling: 2. Application, *Water Resour. Res.*, 42(3), W03408,
1136 doi:10.1029/2005WR004376, 2006b.
- 1137 Koivusalo, H. and Heikinheimo, M.: Surface energy exchange over a boreal snowpack:
1138 comparison of two snow energy balance models, *Hydrol. Process.*, 13(14-15), 2395–2408,
1139 doi:10.1002/(SICI)1099-1085(199910)13:14/15<2395::AID-HYP864>3.0.CO;2-G, 1999.

- 1140 Kuczera, G. and Parent, E.: Monte Carlo assessment of parameter uncertainty in conceptual
1141 catchment models: the Metropolis algorithm, *J. Hydrol.*, 211(1-4), 69–85, doi:10.1016/S0022-
1142 1694(98)00198-X, 1998.
- 1143 Kuczera, G., Renard, B., Thyer, M. and Kavetski, D.: There are no hydrological monsters, just
1144 models and observations with large uncertainties!, *Hydrol. Sci. J.*, 55(6), 980–991,
1145 doi:10.1080/02626667.2010.504677, 2010.
- 1146 Landry, C. C., Buck, K. A., Raleigh, M. S. and Clark, M. P.: Mountain system monitoring at
1147 Senator Beck Basin, San Juan Mountains, Colorado: A new integrative data source to develop
1148 and evaluate models of snow and hydrologic processes, *Water Resour. Res.*, 50,
1149 doi:10.1002/2013WR013711, 2014.
- 1150 Lapo, K. E., Hinkelman, L. M., Raleigh, M. S. and Lundquist, J. D.: Impact of errors in the
1151 downwelling irradiances on simulations of snow water equivalent, snow surface temperature,
1152 and the snow energy balance, *Water Resour. Res.*, 6(4), doi:10.1002/2014WR016259, 2015.
- 1153 Lapp, S., Byrne, J., Townshend, I. and Kienzle, S.: Climate warming impacts on snowpack
1154 accumulation in an alpine watershed, *Int. J. Climatol.*, 25(4), 521–536, doi:10.1002/joc.1140,
1155 2005.
- 1156 Leavesley, G. H.: Modeling the effects of climate change on water resources - a review, *Clim.*
1157 *Change*, 28(1-2), 159–177, doi:10.1007/BF01094105, 1994.
- 1158 Lehning, M., Völksch, I., Gustafsson, D., Nguyen, T. A., Stähli, M. and Zappa, M.: ALPINE3D:
1159 a detailed model of mountain surface processes and its application to snow hydrology, *Hydrol.*
1160 *Process.*, 20, 2111–2128, doi:10.1002/hyp.6204, 2006.
- 1161 Li, J., Duan, Q. Y., Gong, W., Ye, A., Dai, Y., Miao, C., Di, Z., Tong, C. and Sun, Y.: Assessing
1162 parameter importance of the Common Land Model based on qualitative and quantitative
1163 sensitivity analysis, *Hydrol. Earth Syst. Sci.*, 17(8), 3279–3293, doi:10.5194/hess-17-3279-2013,
1164 2013.
- 1165 Liston, G. E.: Representing Subgrid Snow Cover Heterogeneities in Regional and Global
1166 Models, *J. Clim.*, 17(6), 1381–1397, doi:10.1175/1520-
1167 0442(2004)017<1381:RSSCHI>2.0.CO;2, 2004.
- 1168 Liston, G. E. and Elder, K.: A Meteorological Distribution System for High-Resolution
1169 Terrestrial Modeling (MicroMet), *J. Hydrometeorol.*, 7(2), 217–234, doi:10.1175/JHM486.1,
1170 2006.
- 1171 Liu, Y. and Gupta, H. V.: Uncertainty in hydrologic modeling: Toward an integrated data
1172 assimilation framework, *Water Resour. Res.*, 43(7), doi:10.1029/2006WR005756, 2007.

- 1173 Luce, C. H., Tarboton, D. G. and Cooley, K. R.: The influence of the spatial distribution of snow
1174 on basin-averaged snowmelt, *Hydrol. Process.*, 12(10-11), 1671–1683, doi:10.1002/(SICI)1099-
1175 1085(199808/09)12:10/11<1671::AID-HYP688>3.0.CO;2-N, 1998.
- 1176 Lundquist, J. D. and Cayan, D. R.: Surface temperature patterns in complex terrain: Daily
1177 variations and long-term change in the central Sierra Nevada, California, *J. Geophys. Res.*, 112,
1178 D11124, doi:10.1029/2006JD007561, 2007.
- 1179 Lundquist, J. D., Wayand, N. E., Massmann, A., Clark, M. P., Lott, F. and Cristea, N. C.:
1180 Diagnosis of insidious data disasters, *Water Resour. Res.*, 51, doi:10.1002/2014WR016585,
1181 2015.
- 1182 Luo, W., Taylor, M. C. and Parker, S. R.: A comparison of spatial interpolation methods to
1183 estimate continuous wind speed surfaces using irregularly distributed data from England and
1184 Wales, *Int. J. Climatol.*, 28(7), 947–959, doi:10.1002/joc.1583, 2008.
- 1185 Magnusson, J., Wever, N., Essery, R., Helbig, N., Winstral, A. and Jonas, T.: Evaluating snow
1186 models with varying process representations for hydrological applications, *Water Resour. Res.*,
1187 51, doi:10.1002/2014WR016498, 2015.
- 1188 Mahat, V. and Tarboton, D. G.: Canopy radiation transmission for an energy balance snowmelt
1189 model, *Water Resour. Res.*, 48(1), 1–16, doi:10.1029/2011WR010438, 2012.
- 1190 Mardikis, M. G., Kalivas, D. P. and Kollias, V. J.: Comparison of Interpolation Methods for the
1191 Prediction of Reference Evapotranspiration—An Application in Greece, *Water Resour. Manag.*,
1192 19(3), 251–278, doi:10.1007/s11269-005-3179-2, 2005.
- 1193 Marks, D. and Dozier, J.: Climate and energy exchange at the snow surface in the Alpine Region
1194 of the Sierra Nevada: 2. Snow cover energy balance, *Water Resour. Res.*, 28(11), 3043–3054,
1195 doi:10.1029/92WR01483, 1992.
- 1196 Marks, D., Dozier, J. and Davis, R. E.: Climate and energy exchange at the snow surface in the
1197 Alpine Region of the Sierra Nevada: 1. Meteorological measurements and monitoring, *Water*
1198 *Resour. Res.*, 28(11), 3029–3042, doi:10.1029/92WR01482, 1992.
- 1199 Matott, L. S., Babendreier, J. E. and Purucker, S. T.: Evaluating uncertainty in integrated
1200 environmental models: A review of concepts and tools, *Water Resour. Res.*, 45(6),
1201 doi:10.1029/2008WR007301, 2009.
- 1202 Meyer, J. D. D., Jin, J. and Wang, S.-Y.: Systematic Patterns of the Inconsistency between Snow
1203 Water Equivalent and Accumulated Precipitation as Reported by the Snowpack Telemetry
1204 Network, *J. Hydrometeorol.*, 13(6), 1970–1976, doi:10.1175/JHM-D-12-066.1, 2012.
- 1205 Mizukami, N., Clark, M. P., Slater, A. G., Brekke, L. D., Elsner, M. M., Arnold, J. R. and
1206 Gangopadhyay, S.: Hydrologic Implications of Different Large-Scale Meteorological Model

- 1207 Forcing Datasets in Mountainous Regions, *J. Hydrometeorol.*, 15(1), 474–488,
1208 doi:10.1175/JHM-D-13-036.1, 2014.
- 1209 Morin, S., Lejeune, Y., Lesaffre, B., Panel, J.-M., Poncet, D., David, P. and Sudul, M.: An 18-yr
1210 long (1993–2011) snow and meteorological dataset from a mid-altitude mountain site (Col de
1211 Porte, France, 1325 m alt.) for driving and evaluating snowpack models, *Earth Syst. Sci. Data*,
1212 4(1), 13–21, doi:10.5194/essd-4-13-2012, 2012.
- 1213 Morris, M. D.: Factorial Sampling Plans for Preliminary Computational Experiments,
1214 *Technometrics*, 33(2), 161–174, doi:10.1080/00401706.1991.10484804, 1991.
- 1215 Mott, R. and Lehning, M.: Meteorological Modeling of Very High-Resolution Wind Fields and
1216 Snow Deposition for Mountains, *J. Hydrometeorol.*, 11(4), 934–949,
1217 doi:10.1175/2010JHM1216.1, 2010.
- 1218 Niemelä, S., Räisänen, P. and Savijärvi, H.: Comparison of surface radiative flux
1219 parameterizations: Part I. Longwave radiation, *Atmos. Res.*, 58(1), 1–18, doi:10.1016/S0169-
1220 8095(01)00084-9, 2001a.
- 1221 Niemelä, S., Räisänen, P. and Savijärvi, H.: Comparison of surface radiative flux
1222 parameterizations: Part II. Shortwave radiation, *Atmos. Res.*, 58(2), 141–154,
1223 doi:10.1016/S0169-8095(01)00085-0, 2001b.
- 1224 Nossent, J., Elsen, P. and Bauwens, W.: Sobol’ sensitivity analysis of a complex environmental
1225 model, *Environ. Model. Softw.*, 26(12), 1515–1525, doi:10.1016/j.envsoft.2011.08.010, 2011.
- 1226 Oudin, L., Perrin, C., Mathevet, T., Andréassian, V. and Michel, C.: Impact of biased and
1227 randomly corrupted inputs on the efficiency and the parameters of watershed models, *J. Hydrol.*,
1228 320(1-2), 62–83, doi:10.1016/j.jhydrol.2005.07.016, 2006.
- 1229 Pappenberger, F. and Beven, K. J.: Ignorance is bliss: Or seven reasons not to use uncertainty
1230 analysis, *Water Resour. Res.*, 42(W05302), doi:10.1029/2005WR004820, 2006.
- 1231 Pappenberger, F., Beven, K. J., Ratto, M. and Matgen, P.: Multi-method global sensitivity
1232 analysis of flood inundation models, *Adv. Water Resour.*, 31(1), 1–14,
1233 doi:10.1016/j.advwatres.2007.04.009, 2008.
- 1234 Phillips, D. and Marks, D.: Spatial uncertainty analysis: propagation of interpolation errors in
1235 spatially distributed models, *Ecol. Modell.*, 91(1-3), 213–229, doi:10.1016/0304-3800(95)00191-
1236 3, 1996.
- 1237 Rakovec, O., Hill, M. C., Clark, M. P., Weerts, A. H., Teuling, A. J. and Uijlenhoet, R.:
1238 Distributed Evaluation of Local Sensitivity Analysis (DELSA), with application to hydrologic
1239 models, *Water Resour. Res.*, 50, doi:10.1002/2013WR014063, 2014.

- 1240 Raleigh, M. S.: Quantification of uncertainties in snow accumulation, snowmelt, and snow
1241 disappearance dates, University of Washington., 2013.
- 1242 Raleigh, M. S. and Lundquist, J. D.: Comparing and combining SWE estimates from the SNOW-
1243 17 model using PRISM and SWE reconstruction, *Water Resour. Res.*, 48(1),
1244 doi:10.1029/2011WR010542, 2012.
- 1245 Rasmussen, R., Baker, B., Kochendorfer, J., Meyers, T., Landolt, S., Fischer, A. P., Black, J.,
1246 Thériault, J. M., Kucera, P., Gochis, D., Smith, C., Nitu, R., Hall, M., Ikeda, K. and Gutmann,
1247 E.: How Well Are We Measuring Snow: The NOAA/FAA/NCAR Winter Precipitation Test Bed,
1248 *Bull. Am. Meteorol. Soc.*, 93(6), 811–829, doi:10.1175/BAMS-D-11-00052.1, 2012.
- 1249 Rasmussen, R., Ikeda, K., Liu, C., Gochis, D., Clark, M., Dai, A., Gutmann, E., Dudhia, J.,
1250 Chen, F., Barlage, M., Yates, D. and Zhang, G.: Climate Change Impacts on the Water Balance
1251 of the Colorado Headwaters: High-Resolution Regional Climate Model Simulations, *J.*
1252 *Hydrometeorol.*, 15(3), 1091–1116, doi:10.1175/JHM-D-13-0118.1, 2014.
- 1253 Rasmussen, R., Liu, C., Ikeda, K., Gochis, D., Yates, D., Chen, F., Tewari, M., Barlage, M.,
1254 Dudhia, J., Yu, W., Miller, K., Arsenault, K., Grubišić, V., Thompson, G. and Gutmann, E.:
1255 High-Resolution Coupled Climate Runoff Simulations of Seasonal Snowfall over Colorado: A
1256 Process Study of Current and Warmer Climate, *J. Clim.*, 24(12), 3015–3048,
1257 doi:10.1175/2010JCLI3985.1, 2011.
- 1258 Razavi, S. and Gupta, H. V.: What do we mean by sensitivity analysis? The need for
1259 comprehensive characterization of “Global” sensitivity in Earth and Environmental Systems
1260 Models, *Water Resour. Res.*, 51, doi:10.1002/2014WR016527, 2015.
- 1261 Reba, M. L., Marks, D., Seyfried, M., Winstral, A., Kumar, M. and Flerchinger, G.: A long-term
1262 data set for hydrologic modeling in a snow-dominated mountain catchment, *Water Resour. Res.*,
1263 47(7), W07702, doi:10.1029/2010WR010030, 2011.
- 1264 Refsgaard, J. C., van der Sluijs, J. P., Brown, J. and van der Keur, P.: A framework for dealing
1265 with uncertainty due to model structure error, *Adv. Water Resour.*, 29(11), 1586–1597,
1266 doi:10.1016/j.advwatres.2005.11.013, 2006.
- 1267 Rosero, E., Yang, Z.-L., Wagener, T., Gulden, L. E., Yatheendradas, S. and Niu, G.-Y.:
1268 Quantifying parameter sensitivity, interaction, and transferability in hydrologically enhanced
1269 versions of the Noah land surface model over transition zones during the warm season, *J.*
1270 *Geophys. Res.*, 115, D03106, doi:10.1029/2009JD012035, 2010.
- 1271 Rosolem, R., Gupta, H. V., Shuttleworth, W. J., Zeng, X. and de Gonçalves, L. G. G.: A fully
1272 multiple-criteria implementation of the Sobol’ method for parameter sensitivity analysis, *J.*
1273 *Geophys. Res. Atmos.*, 117, D07103, doi:10.1029/2011JD016355, 2012.
- 1274 Saltelli, A.: Sensitivity analysis: Could better methods be used?, *J. Geophys. Res.*, 104(D3),
1275 3789, doi:10.1029/1998JD100042, 1999.

- 1276 Saltelli, A. and Annoni, P.: How to avoid a perfunctory sensitivity analysis, *Environ. Model.*
1277 *Softw.*, 25(12), 1508–1517, doi:10.1016/j.envsoft.2010.04.012, 2010.
- 1278 Saltelli, A., Annoni, P., Azzini, I., Campolongo, F., Ratto, M. and Tarantola, S.: Variance based
1279 sensitivity analysis of model output. Design and estimator for the total sensitivity index, *Comput.*
1280 *Phys. Commun.*, 181(2), 259–270, doi:10.1016/j.cpc.2009.09.018, 2010.
- 1281 Sauter, T. and Obleitner, F.: Assessment of the uncertainty of snowpack simulations based on
1282 variance decomposition, *Geosci. Model Dev. Discuss.*, 8(3), 2807–2845, doi:10.5194/gmdd-8-
1283 2807-2015, 2015.
- 1284 Schmucki, E., Marty, C., Fierz, C. and Lehning, M.: Evaluation of modelled snow depth and
1285 snow water equivalent at three contrasting sites in Switzerland using SNOWPACK simulations
1286 driven by different meteorological data input, *Cold Reg. Sci. Technol.*, 99, 27–37,
1287 doi:10.1016/j.coldregions.2013.12.004, 2014.
- 1288 Serreze, M. C., Clark, M. P., Armstrong, R. L., McGinnis, D. A. and Pulwarty, R. S.:
1289 Characteristics of the western United States snowpack from snowpack telemetry (SNOTEL)
1290 data, *Water Resour. Res.*, 35(7), 2145–2160, doi:10.1029/1999WR900090, 1999.
- 1291 Shamir, E. and Georgakakos, K. P.: Distributed snow accumulation and ablation modeling in the
1292 American River basin, *Adv. Water Resour.*, 29, 558–570, doi:10.1016/j.advwatres.2005.06.010,
1293 2006.
- 1294 Skiles, S. M., Painter, T. H., Deems, J. S., Bryant, A. C. and Landry, C. C.: Dust radiative
1295 forcing in snow of the Upper Colorado River Basin: 2. Interannual variability in radiative forcing
1296 and snowmelt rates, *Water Resour. Res.*, 48(7), doi:10.1029/2012WR011986, 2012.
- 1297 Slater, A. G. and Clark, M. P.: Snow Data Assimilation via an Ensemble Kalman Filter, *J.*
1298 *Hydrometeorol.*, 7(3), 478–493, doi:10.1175/JHM505.1, 2006.
- 1299 Slater, A. G., Schlosser, C. A., Desborough, C. E., Pitman, A. J., Henderson-Sellers, A., Robock,
1300 A., Vinnikov, K. Y., Entin, J., Mitchell, K., Chen, F., Boone, A., Etchevers, P., Habets, F.,
1301 Noilhan, J., Braden, H., Cox, P. M., de Rosnay, P., Dickinson, R. E., Yang, Z.-L., Dai, Y.-J.,
1302 Zeng, Q., Duan, Q., Koren, V., Schaake, S., Gedney, N., Gusev, Y. M., Nasonova, O. N., Kim,
1303 J., Kowalczyk, E. A., Shmakin, A. B., Smirnova, T. G., Verseghy, D., Wetzell, P. and Xue, Y.:
1304 The Representation of Snow in Land Surface Schemes: Results from PILPS 2(d), *J.*
1305 *Hydrometeorol.*, 2(1), 7–25, doi:10.1175/1525-7541(2001)002<0007:TROSIL>2.0.CO;2, 2001.
- 1306 Smith, P. J., Beven, K. J. and Tawn, J. A.: Detection of structural inadequacy in process-based
1307 hydrological models: A particle-filtering approach, *Water Resour. Res.*, 44(1), W01410,
1308 doi:10.1029/2006WR005205, 2008.
- 1309 Sobol', I.: On sensitivity estimation for nonlinear mathematical models, *Mat. Model.*, 2(1), 112–
1310 118, 1990.

- 1311 Song, X., Zhang, J., Zhan, C., Xuan, Y., Ye, M. and Xu, C.: Global sensitivity analysis in
1312 hydrological modeling: Review of concepts, methods, theoretical framework, and applications, *J.*
1313 *Hydrol.*, 523(225), 739–757, doi:10.1016/j.jhydrol.2015.02.013, 2015.
- 1314 Spank, U., Schwärzel, K., Renner, M., Moderow, U. and Bernhofer, C.: Effects of measurement
1315 uncertainties of meteorological data on estimates of site water balance components, *J. Hydrol.*,
1316 492, 176–189, doi:10.1016/j.jhydrol.2013.03.047, 2013.
- 1317 Sturm, M., Holmgren, J. and Liston, G. E.: A Seasonal Snow Cover Classification System for
1318 Local to Global Applications, *J. Clim.*, 8(5), 1261–1283, doi:10.1175/1520-
1319 0442(1995)008<1261:ASSCCS>2.0.CO;2, 1995.
- 1320 Sturm, M. and Wagner, A. M.: Using repeated patterns in snow distribution modeling: An Arctic
1321 example, *Water Resour. Res.*, 46(12), 1–15, doi:10.1029/2010WR009434, 2010.
- 1322 Tang, Y., Reed, P., Wagener, T. and van Werkhoven, K.: Comparing sensitivity analysis
1323 methods to advance lumped watershed model identification and evaluation, *Hydrol. Earth Syst.*
1324 *Sci.*, 11(2), 793–817, doi:10.5194/hess-11-793-2007, 2007.
- 1325 Tarboton, D. and Luce, C.: Utah Energy Balance Snow Accumulation and Melt Model (UEB), in
1326 Computer model technical description users guide, Utah Water Res. Lab. and USDA For. Serv.
1327 Intermt. Res. Station, p. 64, Logan, UT., 1996.
- 1328 Thornton, P. E., Hasenauer, H. and White, M. A.: Simultaneous estimation of daily solar
1329 radiation and humidity from observed temperature and precipitation: an application over
1330 complex terrain in Austria, *Agric. For. Meteorol.*, 104(4), 255–271, doi:10.1016/S0168-
1331 1923(00)00170-2, 2000.
- 1332 Touhami, H. Ben, Lardy, R., Barra, V. and Bellocchi, G.: Screening parameters in the Pasture
1333 Simulation model using the Morris method, *Ecol. Modell.*, 266(1), 42–57,
1334 doi:10.1016/j.ecolmodel.2013.07.005, 2013.
- 1335 Trujillo, E. and Molotch, N. P.: Snowpack regimes of the Western United States, *Water Resour.*
1336 *Res.*, 50, doi:10.1002/2013WR014753, 2014.
- 1337 Vrugt, J. A., Braak, C. J. F., Gupta, H. V. and Robinson, B. A.: Equifinality of formal (DREAM)
1338 and informal (GLUE) Bayesian approaches in hydrologic modeling?, *Stoch. Environ. Res. Risk*
1339 *Assess.*, 23(7), 1011–1026, doi:10.1007/s00477-008-0274-y, 2008a.
- 1340 Vrugt, J. A., ter Braak, C. J. F., Clark, M. P., Hyman, J. M. and Robinson, B. A.: Treatment of
1341 input uncertainty in hydrologic modeling: Doing hydrology backward with Markov chain Monte
1342 Carlo simulation, *Water Resour. Res.*, 44(12), doi:10.1029/2007WR006720, 2008b.
- 1343 Vrugt, J. A., Diks, C. G. H., Gupta, H. V., Bouten, W. and Verstraten, J. M.: Improved treatment
1344 of uncertainty in hydrologic modeling: Combining the strengths of global optimization and data
1345 assimilation, *Water Resour. Res.*, 41(1), W01017, doi:10.1029/2004WR003059, 2005.

- 1346 Vrugt, J. A., Gupta, H. V., Bastidas, L. A., Bouten, W. and Sorooshian, S.: Effective and
1347 efficient algorithm for multiobjective optimization of hydrologic models, *Water Resour. Res.*,
1348 39(8), doi:10.1029/2002WR001746, 2003a.
- 1349 Vrugt, J. A., Gupta, H. V., Bouten, W. and Sorooshian, S.: A Shuffled Complex Evolution
1350 Metropolis algorithm for optimization and uncertainty assessment of hydrologic model
1351 parameters, *Water Resour. Res.*, 39(8), doi:10.1029/2002WR001642, 2003b.
- 1352 Wayand, N. E., Hamlet, A. F., Hughes, M., Feld, S. I. and Lundquist, J. D.: Intercomparison of
1353 Meteorological Forcing Data from Empirical and Mesoscale Model Sources in the N.F.
1354 American River Basin in northern Sierra Nevada, California, *J. Hydrometeorol.*, 14(3), 677–699,
1355 doi:10.1175/JHM-D-12-0102.1, 2013.
- 1356 Van Werkhoven, K., Wagener, T., Reed, P. and Tang, Y.: Characterization of watershed model
1357 behavior across a hydroclimatic gradient, *Water Resour. Res.*, 44(1), W01429,
1358 doi:10.1029/2007WR006271, 2008.
- 1359 Winstral, A. and Marks, D.: Simulating wind fields and snow redistribution using terrain-based
1360 parameters to model snow accumulation and melt over a semi-arid mountain catchment, *Hydrol.*
1361 *Process.*, 16(18), 3585–3603, doi:10.1002/hyp.1238, 2002.
- 1362 Winstral, A., Marks, D. and Gurney, R.: An efficient method for distributing wind speeds over
1363 heterogeneous terrain, *Hydrol. Process.*, 23, 2526–2535, doi:10.1002/hyp.7141, 2009.
- 1364 Winstral, A., Marks, D. and Gurney, R.: Simulating wind-affected snow accumulations at
1365 catchment to basin scales, *Adv. Water Resour.*, 55, 64–79, doi:10.1016/j.advwatres.2012.08.011,
1366 2013.
- 1367 Xia, Y., Yang, Z.-L., Stoffa, P. L. and Sen, M. K.: Using different hydrological variables to
1368 assess the impacts of atmospheric forcing errors on optimization and uncertainty analysis of the
1369 CHASM surface model at a cold catchment, *J. Geophys. Res.*, 110(D1), D01101,
1370 doi:10.1029/2004JD005130, 2005.
- 1371 Yang, D., Kane, D. L., Hinzman, L. D., Goodison, B. E., Metcalfe, J. R., Louie, P. Y. T.,
1372 Leavesley, G. H., Emerson, D. G. and Hanson, C. L.: An evaluation of the Wyoming Gauge
1373 System for snowfall measurement, *Water Resour. Res.*, 36(9), 2665–2677,
1374 doi:10.1029/2000WR900158, 2000.
- 1375 Yilmaz, K. K., Gupta, H. V. and Wagener, T.: A process-based diagnostic approach to model
1376 evaluation: Application to the NWS distributed hydrologic model, *Water Resour. Res.*, 44,
1377 W09417, doi:10.1029/2007WR006716, 2008.
- 1378 You, J., Tarboton, D. G. and Luce, C. H.: Modeling the snow surface temperature with a one-
1379 layer energy balance snowmelt model, *Hydrol. Earth Syst. Sci. Discuss.*, 10(12), 15071–15118,
1380 doi:10.5194/hessd-10-15071-2013, 2013.

1381 Zuzel, J. F. and Cox, L. M.: Relative importance of meteorological variables in snowmelt, Water
1382 Resour. Res., 11(1), 174–176, doi:10.1029/WR011i001p00174, 1975.

1383

1384 7. Tables

1385 **Table 1** Basic characteristics of the snow study sites, ordered from left-to-right by increasing elevation.

Site Name	Innavait Creek	Col de Porte	Reynolds Mountain East (sheltered site)	Swamp Angel Study Plot
Site ID	IC	CDP	RME	SASP
Location	Alaska, USA	Rhône-Alpes, France	Idaho, USA	Colorado, USA
Latitude (N)	68.62	45.30	43.07	37.91
Longitude (E)	-149.30	5.77	-116.75	-107.71
Elevation (m)	930	1330	2060	3370
Study Period (WY)	2011	2006	2007	2008
Snow Climate	Tundra	Mountain (maritime)	Mountain (intermountain)	Mountain (continental)
Sensors	T_{air} : Vaisala HMP45C P : Campbell Scientific TE 525 U : Met One 014A RH : Vaisala HMP45C Q_{si} : Kipp & Zonen CMA 6 Q_{li} : none (taken as residual from measurements of all other radiation components ^A)	T_{air} : PT 100/4 wires P : PG2000, GEONOR U : Chauvin Arnoux Tavid 87 – non-heated RH : Vaisala HMP 45D Q_{si} : Kipp & Zonen CM14 Q_{li} : Eppley PIR	T_{air} : Vaisala HMP 45 P : Belfort Universal Gages U : Met One 013/023 RH : Vaisala HMP 45 Q_{si} : Eppley Precision Spectral Pyranometer Q_{li} : Eppley PIR	T_{air} : Vaisala CS500 P : ETI Noah II U : RM Young Wind Monitor 05103-5 RH : Vaisala CS500 Q_{si} : Kipp & Zonen CM21 Q_{li} : Kipp & Zonen CG-4
Operators	NRCS, CRREL, Ameriflux	Météo-France	Northwest Watershed Research Center, Agricultural Research Service	Center for Snow and Avalanche Studies
Oct-Dec T_{air} (°C)	-16.1	2.0	0.2	-3.7
Jan-Mar T_{air} (°C)	-14.7	-1.6	-2.0	-8.7
Apr-Jun T_{air} (°C)	-1.4	8.9	8.4	2.7
Oct-Mar P^B (mm)	200	690	480	1000
Mean annual U (m s ⁻¹)	2.2	1.0	1.6	1.1

1386 ^A At IC, Q_{li} was taken as $Q_{\text{li}} = Q_{\text{net}} - (Q_{\text{si}} - Q_{\text{so}}) + (5.67 \times 10^{-8}) T_{\text{surf}}^4$, where Q_{net} is measured net radiation (W m⁻²), Q_{si} is measured incoming shortwave radiation
1387 (W m⁻²), Q_{so} is measured reflected shortwave radiation (W m⁻²), and T_{surf} is measured snow surface temperature (°C).

1388 ^B Note that precipitation data were adjusted with a multiplier (see Section 2) prior to conducting the sensitivity analysis.

1389

1390 **Table 2** UEB model parameters used across all simulations and sites

Description of parameter	Units	Value
Rain threshold temperature	°C	+3.0
Snow threshold temperature	°C	-1.0
Snow emissivity	--	0.99
Bulk snow density	kg m ⁻³	300
Liquid water holding capacity	fraction	0.05
Snow saturated hydraulic conductivity	m hr ⁻¹	20
Visual new snow albedo	--	0.85
Near infrared new snow albedo	--	0.65
New snow threshold depth to reset albedo	m	0.01
Snow surface roughness	m	0.005
Forest canopy fraction	fraction	0
Ground heat flux	W m ⁻²	0

1391 **Table 3** Details of error types, distributions, and uncertainty ranges for the five scenarios. Bold
 1392 face in the error type, distribution, and uncertainty range indicates defining characteristics,
 1393 relative to scenario NB.

Forcing	Error Type ^A	Distribution ^B	Range	Units	Citations and Notes
Scenario NB (k=6, N=10000)					
T_{air}	B	Normal	[-3.0, +3.0]	°C	Bolstad et al. (1998); Chuanyan et al. (2005); Fridley (2009); Hasenauer et al. (2003)
P	B	Lognormal	[-75, +300] ^C	%	Goodison et al. (1998); Luce et al. (1998); Rasmussen et al. (2012); Winstral and Marks (2002)
U	B	Normal	[-3.0, +3.0]	m s ⁻¹	Winstral et al. (2009)
RH	B	Normal	[-25, +25]	%	Bohn et al. (2013); Déry and Stieglitz (2002); Feld et al. (2013)
Q_{si}	B	Normal	[-100, +100]	W m ⁻²	Bohn et al. (2013); Jepsen et al. (2012); Jing and Cess (1998); Niemelä et al. (2001b)
Q_{li}	B	Normal	[-25, +25]	W m ⁻²	Bohn et al. (2013); Flerchinger et al. (2009); Herrero and Polo (2012); Niemelä et al. (2001a)
Scenario NB+RE (k=12, N=10000)					
This scenario has six bias parameters (identical to NB above), plus the following six random error parameters					
T_{air}	RE	Normal	[0.0, 7.5]	°C	Chuanyan et al. (2005); Fridley (2009); Hasenauer et al. (2003); Huwald et al. (2009); Phillips and Marks (1996)
P	RE	Lognormal	[0.0, 25]	%	Guan et al. (2005); Hasenauer et al. (2003); Hutchinson et al. (2009)
U	RE	Normal	[0.0, 5]	m s ⁻¹	Cheng and Georgakakos (2011); Liston and Elder (2006); Luo et al. (2008); Winstral et al. (2009)
RH	RE	Normal	[0.0, 15]	%	Bohn et al. (2013); Liston and Elder (2006); Phillips and Marks (1996)
Q_{si}	RE	Normal	[0.0, 160]	W m ⁻²	Hasenauer et al. (2003); Jepsen et al. (2012); Liston and Elder (2006); Thornton et al. (2000)
Q_{li}	RE	Normal	[0.0, 80]	W m ⁻²	Bohn et al. (2013); Flerchinger et al. (2009); Liston and Elder (2006)
Scenario UB (k=6, N=10000)					
Identical to NB, except all probability distributions are uniform					
Scenario NB_gauge (k=6, N=10000)					
Identical to NB, except P uncertainty mimics documented differences between P and SWE at SNOTEL sites					
P	B	Lognormal	[-10, +10]	%	Meyer et al. (2012)
Scenario NB_lab^D (k=6, N=10000)					
T_{air}	B	Normal	[-0.30, +0.30]	°C	Vaisala HMP45 specified accuracy
P	B	Lognormal	[-3.0, +3.0]^E	%	RM Young 52202 specified accuracy
U	B	Normal	[-0.30, +0.30]	m s ⁻¹	RM Young 05103 specified accuracy
RH	B	Normal	[-3.0, +3.0]	%	Vaisala HMP45 specified accuracy
Q_{si}	B	Normal	[-25, +25]	W m ⁻²	Li-Cor 200X specified accuracy of ~5%
Q_{li}	B	Normal	[-15, +15]	W m ⁻²	Assumed ~5% of mean intersite values

1394 ^A B=bias, RE=random errors. Biases are additive ($b_i=0$, Eq. 5) for all forcings except P , which has multiplicative
 1395 bias ($b_i=1$).

1396 ^B Probability distributions were truncated in instances when introduction of errors caused non-physical forcing
 1397 values (see Sec. 3.3.5).

1398 ^C The high upper P bias (300%) mimics cases where snowfall data collected in an area of drift deposition are
 1399 assumed (incorrectly) to represent other basin locations.

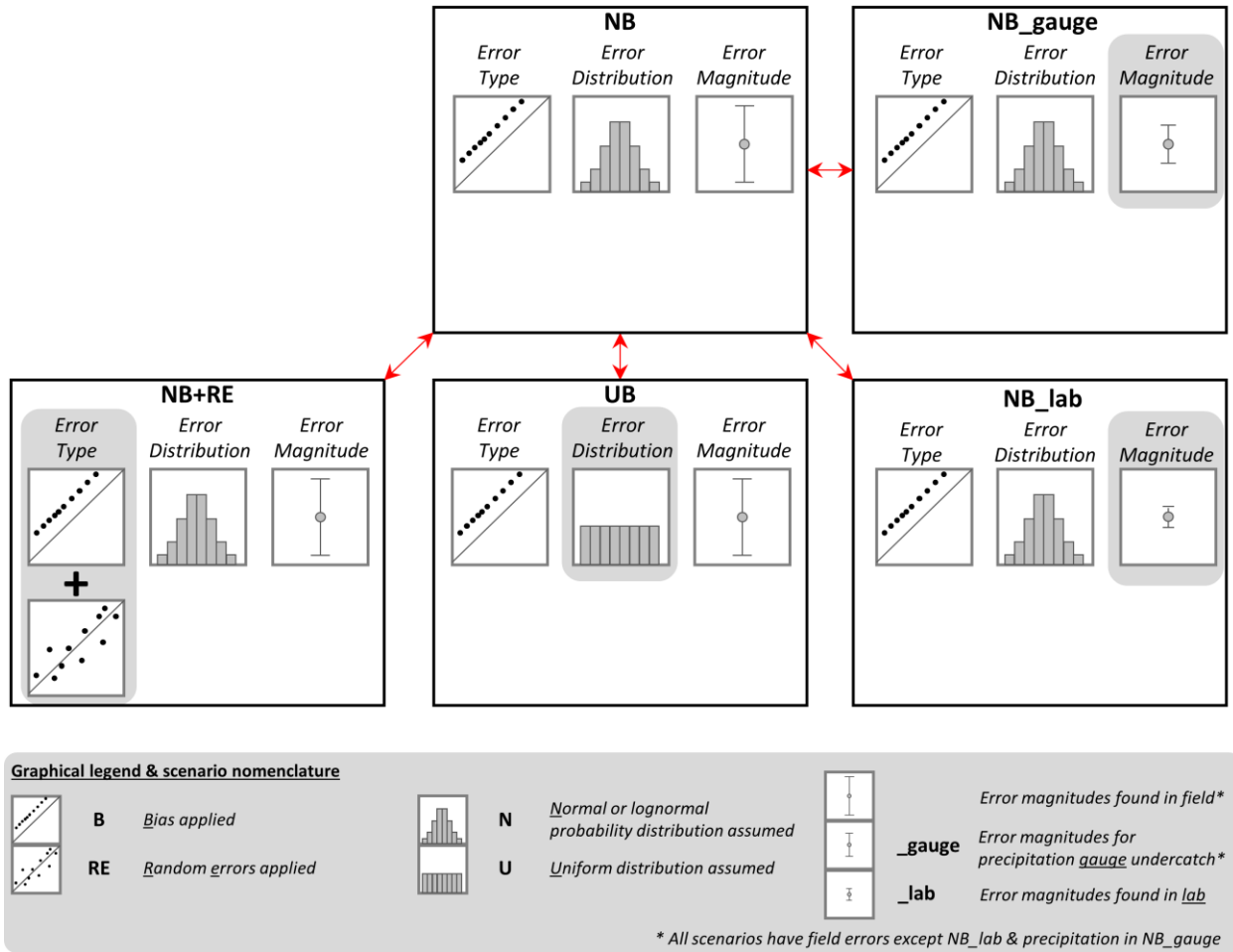
1400 ^D Uncertainty ranges in this scenario are based primarily on manufacturer's specified accuracy for typical sensors
 1401 deployed at SNOTEL sites (*NRCS Staff, personal communication, 2013*). We assume the P storage gauge has the
 1402 same accuracy as a typical tipping bucket gauge.

1403 ^E We neglect P undercatch errors in the lab uncertainty scenario.

1404 **Table 4** Number of samples (model simulations) meeting the requirements for minimum peak
 1405 SWE and snow duration and valid snow disappearance dates at each site in each scenario.

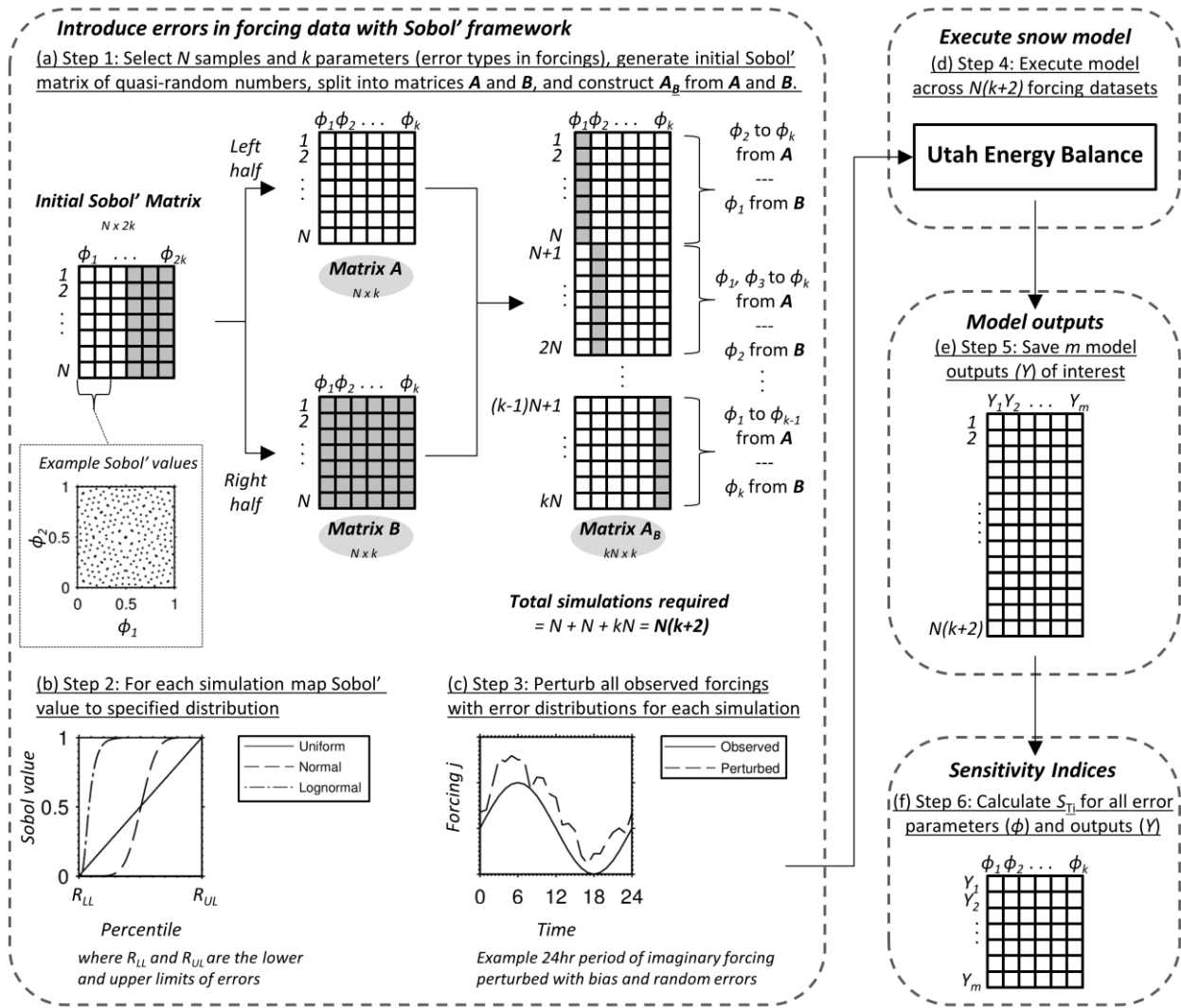
	Scenario NB	Scenario NB+RE	Scenario UB	Scenario NB_gauge	Scenario NB_lab
IC	9898 (79 184)	10 000 (140 000)	8608 (68 864)	10 000 (80 000)	10 000 (80 000)
CDP	9792 (78 336)	9869 (138 166)	8925 (71 400)	9999 (79 992)	10 000 (80 000)
RME	8799 (70 392)	9233 (129 262)	9102 (72 816)	10 000 (80 000)	10 000 (80 000)
SASP	9984 (79 872)	9984 (139 776)	3399 (27 192)	10 000 (80 000)	10 000 (80 000)

1406 **8. Figures**



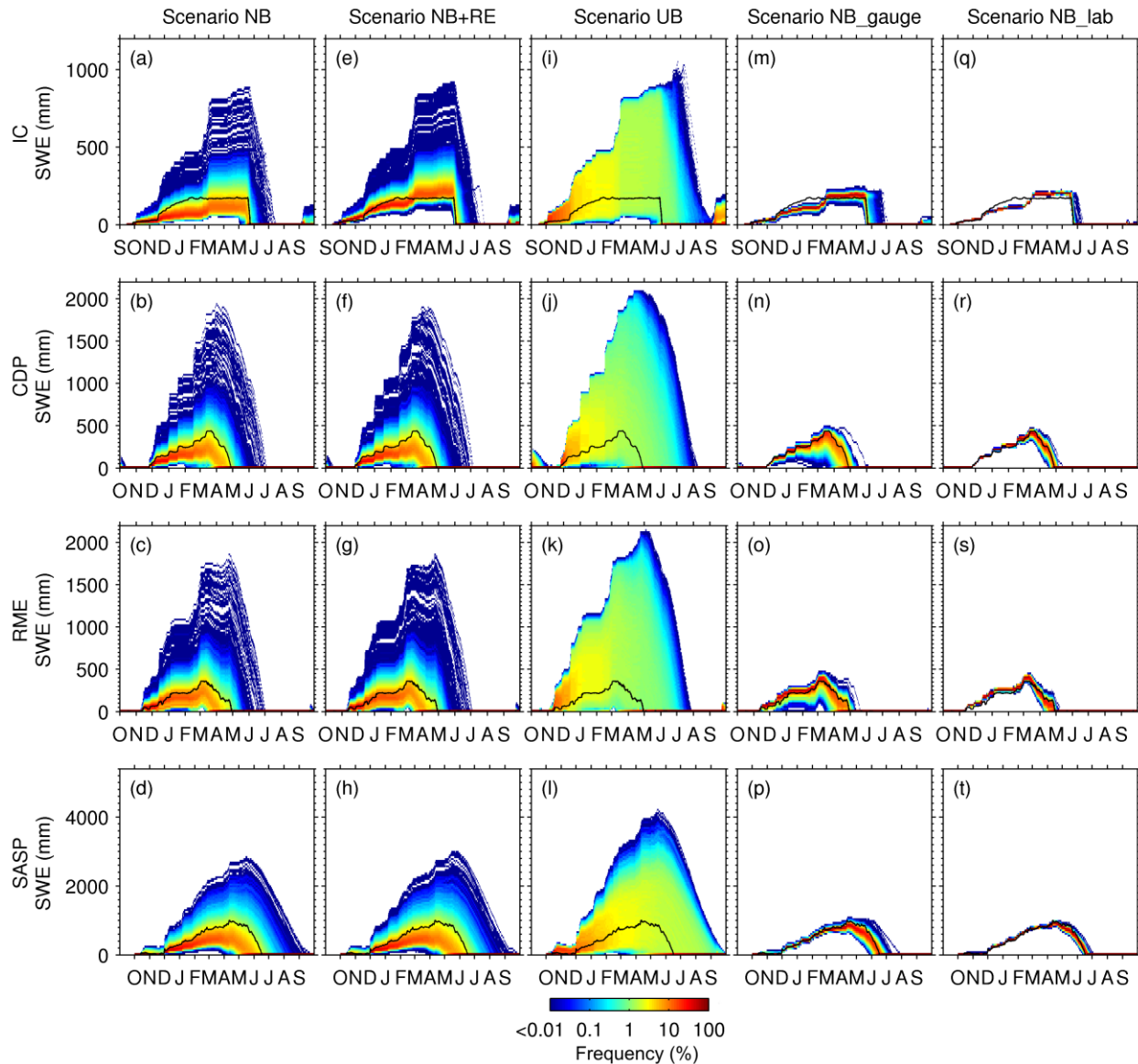
1407

1408 **Figure 1** Scenarios of interest and the type, distribution, and magnitude of errors considered in
 1409 each. NB considers normally (or lognormally) distributed biases with error magnitudes found in
 1410 the field. NB+RE is the same as NB but also considers random errors. UB is the same as NB
 1411 but considers uniformly distributed errors instead. NB_gauge is the same as NB but with
 1412 reduced precipitation uncertainty (typical difference between precipitation gauge and snow
 1413 pillow). NB_lab is the same as NB but considers laboratory error magnitudes.



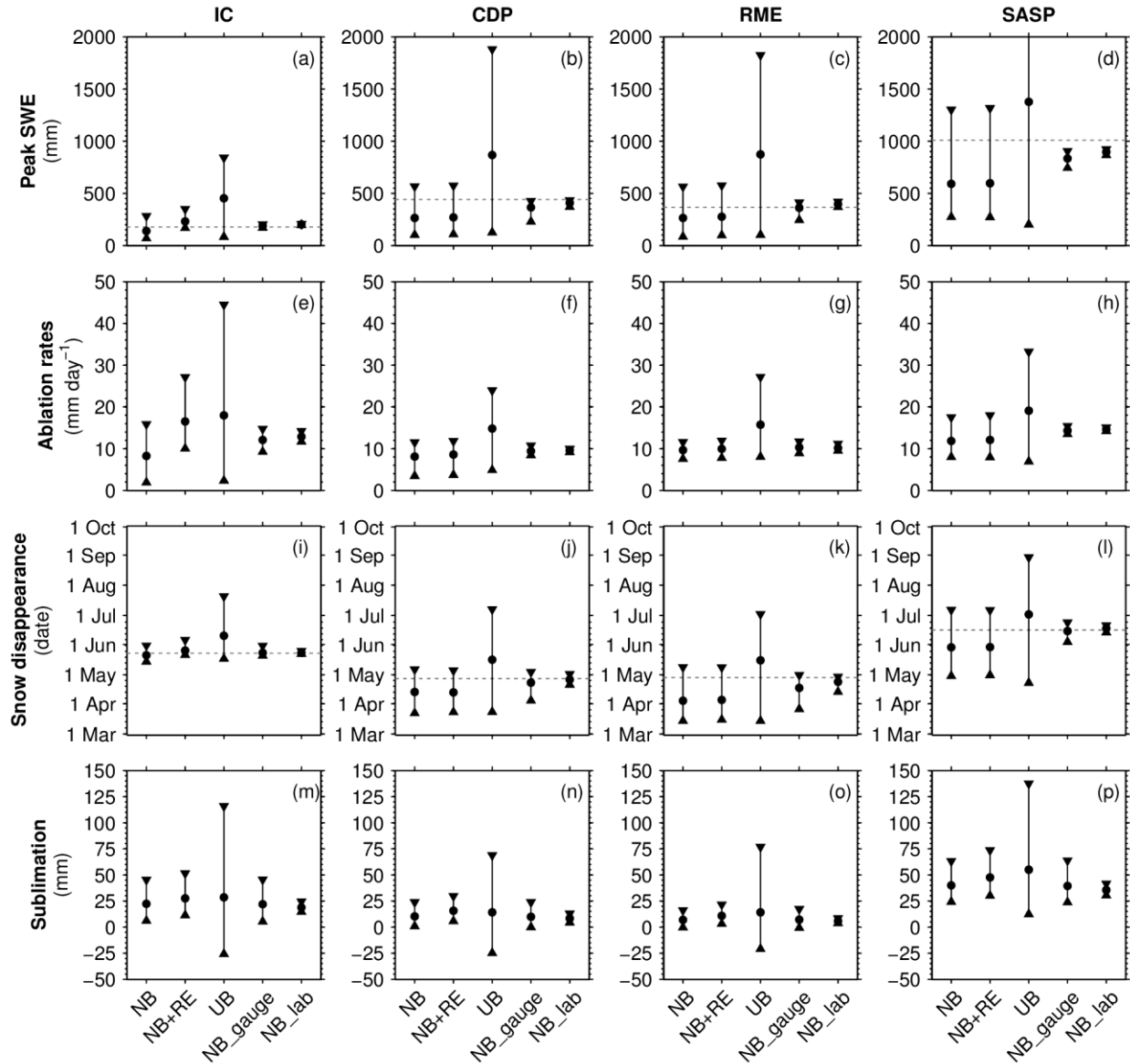
1414

1415 **Figure 2** Conceptual diagram showing methodology for imposing errors on the forcings with
 1416 error parameters (ϕ) within the Sobol' sensitivity analysis framework, and workflow for model
 1417 execution and calculation of sensitivity indices on model outputs (Y).



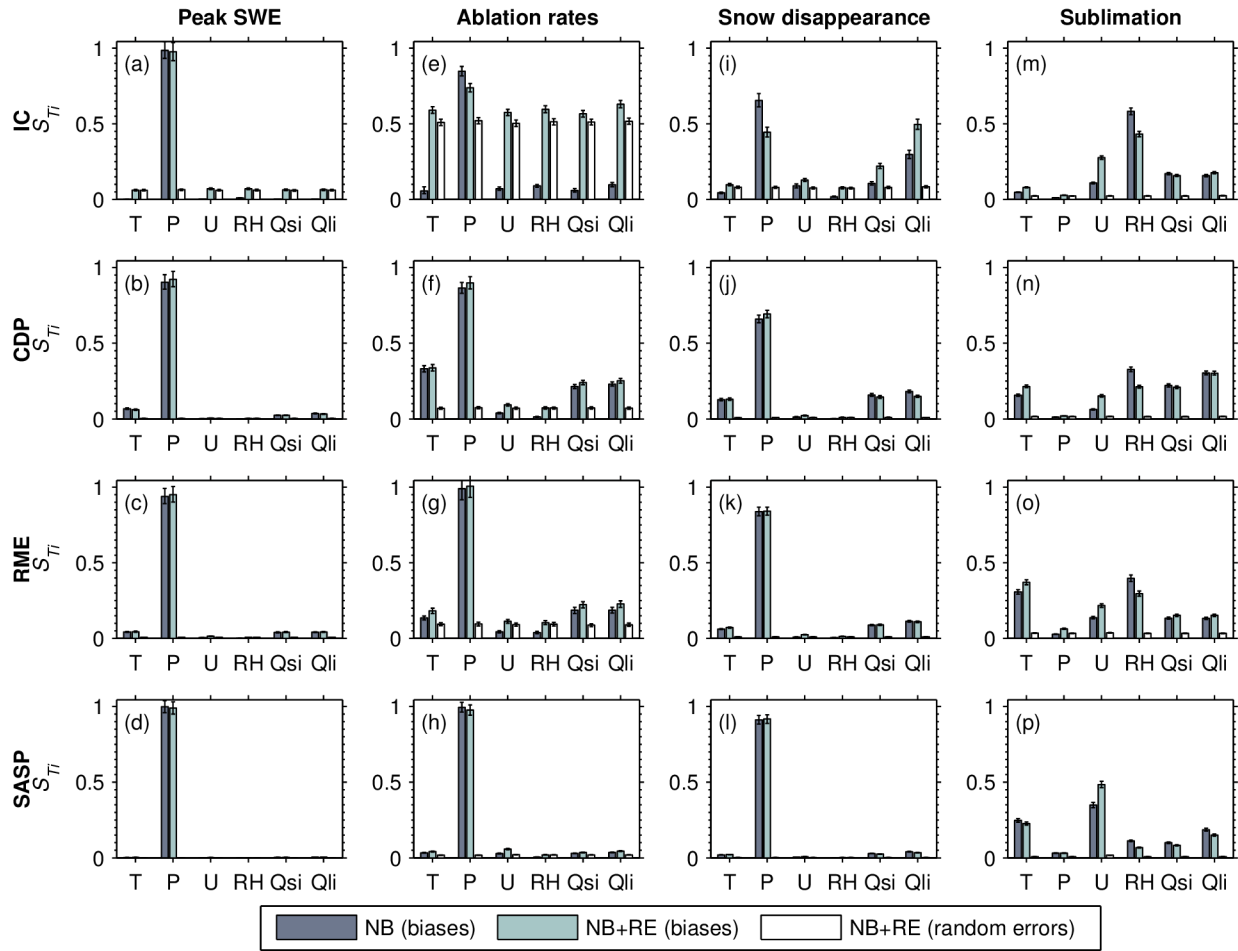
1418

1419 **Figure 3** Observed (black line) and modeled SWE (color density plot) at the four sites across the
 1420 five uncertainty scenarios (see Figure 1 and Table 3). The number of model simulations in the
 1421 density plots varies with the site and scenario (see Table 4). The density plots were constructed
 1422 using 100 bins in the SWE dimension with relative frequency tabulated in each bin each day.
 1423 Note the frequency colorbar is on a logarithmic scale. Sites are arranged from top to bottom in
 1424 order of increasing elevation and decreasing latitude. Scenarios are defined as normally
 1425 distributed bias (NB), normally distributed bias and random errors (NB+RE), uniformly
 1426 distributed bias (UB), normally distributed bias with precipitation gauge uncertainty NB_gauge),
 1427 and normally distributed bias at laboratory error magnitudes (NB_lab).



1428

1429 **Figure 4** Distributions of model outputs (rows) at the four study sites (columns) arranged by
 1430 scenario. For each scenario, the circle is the mean and the whiskers show the range
 1431 encompassing 95% of the simulations (see Table 4 for number of simulations for each site and
 1432 scenario). The dashed lines in (a-d) and (i-l) are the observed values. Axes are matched between
 1433 sites for a given model output; note that the range in scenario UB in (d) is truncated by the axes
 1434 limits (upper value = 3030 mm). Scenarios are defined as normally distributed bias (NB),
 1435 normally distributed bias and random errors (NB+RE), uniformly distributed bias (UB),
 1436 normally distributed bias with precipitation gauge uncertainty NB_gauge), and normally
 1437 distributed bias at laboratory error magnitudes (NB_lab).



1438

1439

1440

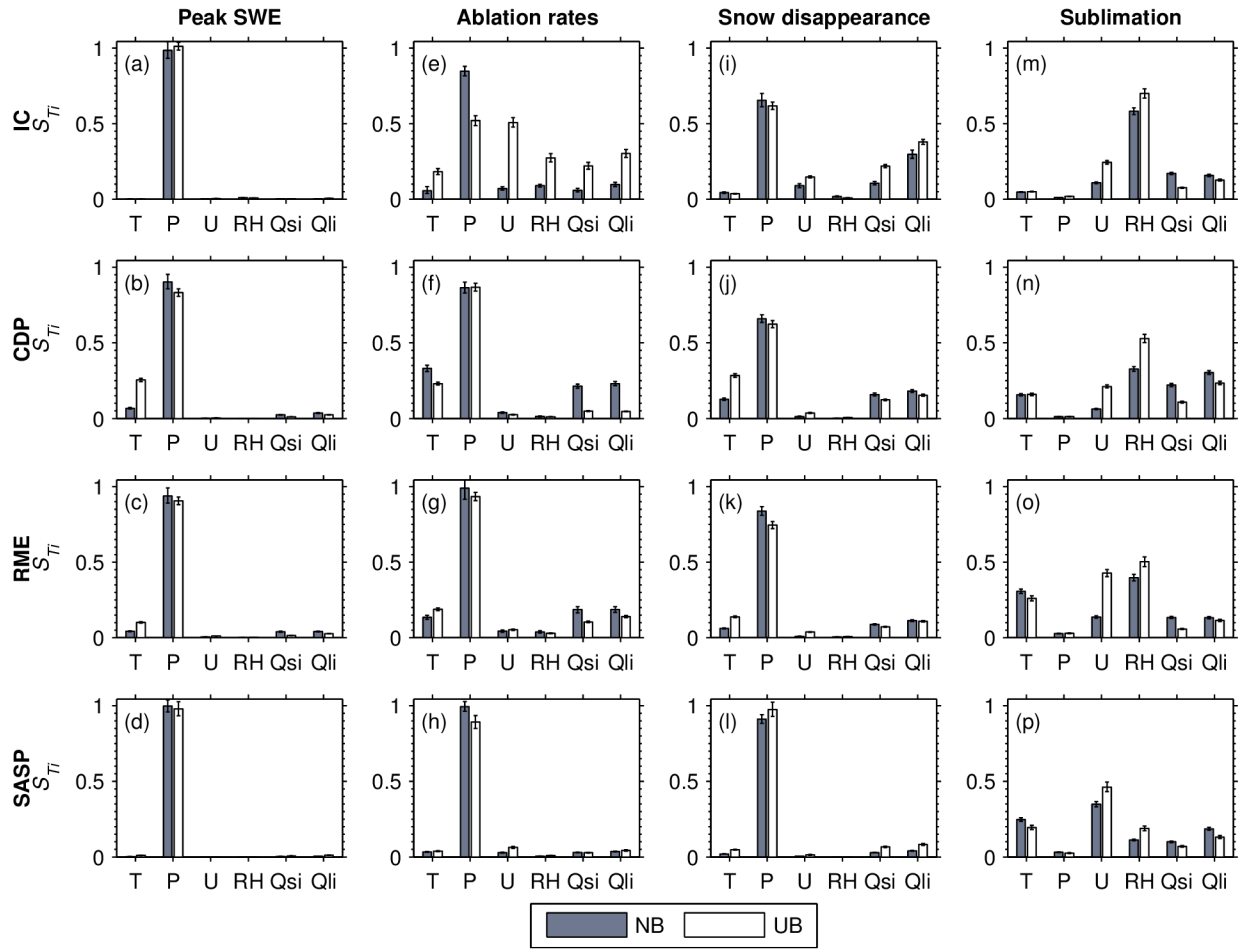
1441

1442

1443

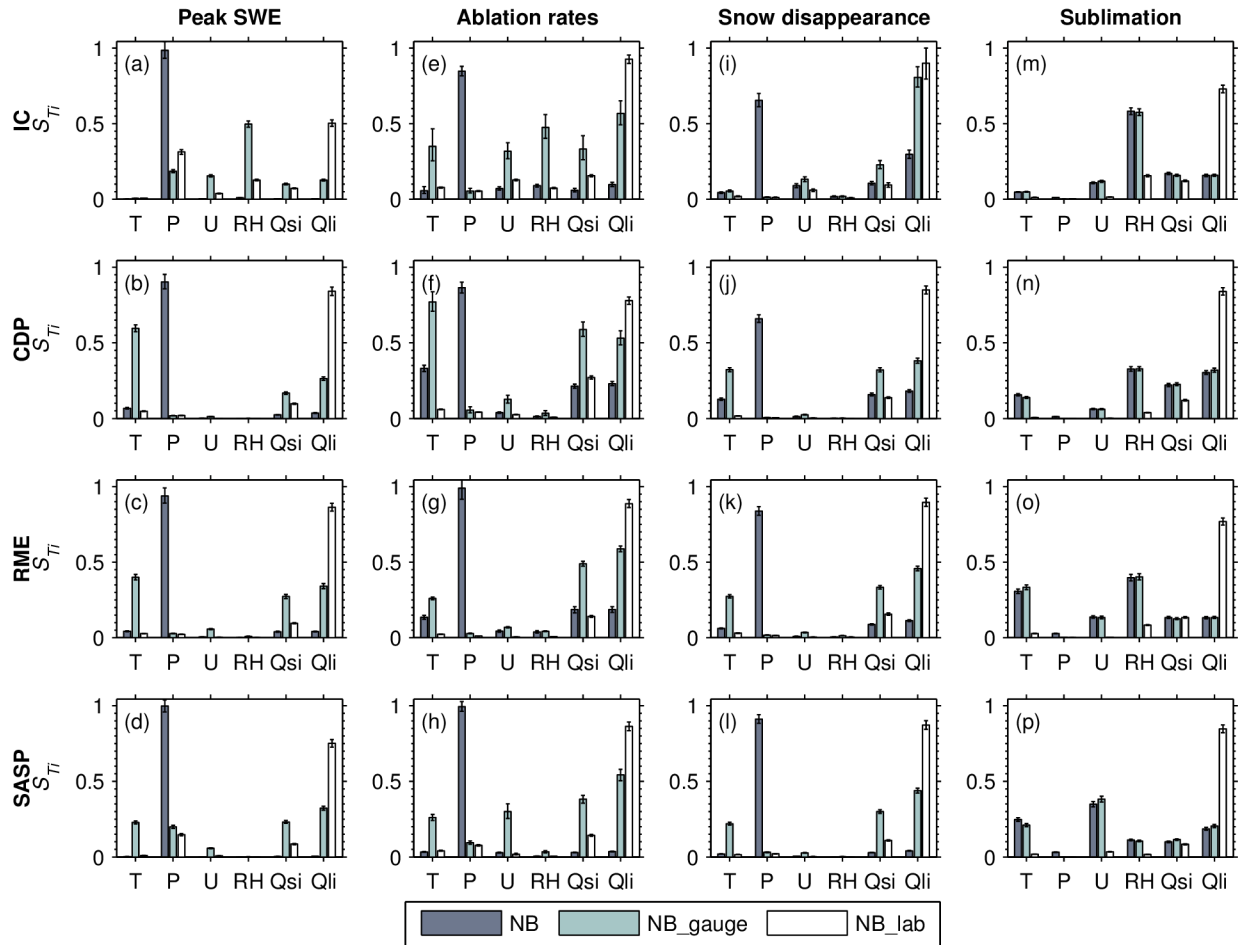
1444

Figure 5 Model sensitivity as a function of forcing error type. Shown are the total-order sensitivity indices (S_{Ti}) of four model response variables (columns) at the four sites (rows) from scenarios NB and NB+RE. In NB+RE, bias and random error parameters are shown separately. NB+RE considers normally distributed bias and random errors, while NB considers normally distributed bias only. The bar indicates the mean (bootstrapped) sensitivity indices and associated 95% confidence intervals.



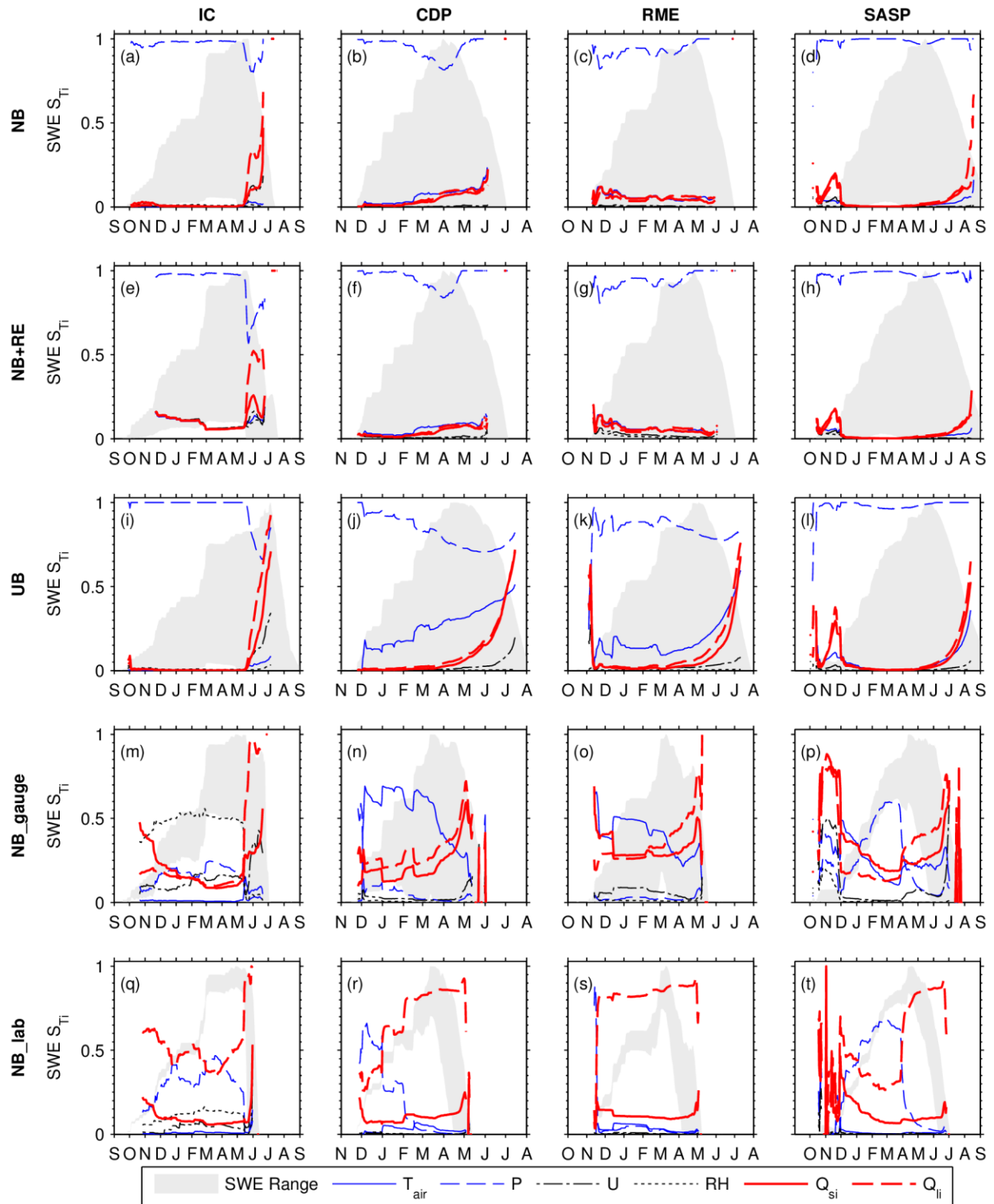
1445
 1446
 1447
 1448

Figure 6 Same as Fig. 5, but comparing S_{Ti} values from scenarios NB and UB to test model sensitivity as a function of error distribution. UB considers uniformly distributed bias, while NB considers normally distributed bias.



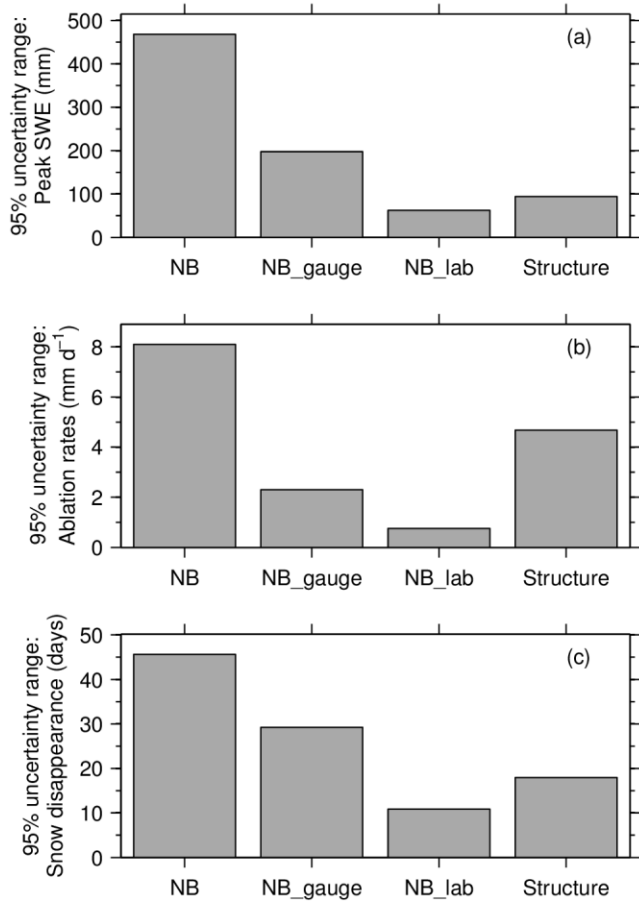
1449
 1450
 1451
 1452
 1453
 1454

Figure 7 Same as Fig. 5, but comparing S_{Ti} values from scenarios NB, NB_gauge, and NB_lab to test model sensitivity as a function of error magnitudes. NB considers normally distributed bias at error magnitudes found in the field. NB_gauge has lower precipitation uncertainty (gauge undercatch) than NB but is otherwise identical. NB_lab considers normally distributed bias at error magnitudes found in the laboratory.



1455

1456 **Figure 8** Variation of daily SWE sensitivity to forcing bias based on site (columns) and error
 1457 scenario (rows). The normalized range (where 1 = maximum SWE) in modeled SWE is shown
 1458 (gray area) for context. Sensitivity indices in the early and late part of the snow season were
 1459 screened out, as a high number of simulations with SWE=0 yielded invalid sensitivity indices.



1460

1461 **Figure 9** Uncertainty ranges (95% intervals) in (a) peak SWE, (b) ablation rates, and (c) snow
 1462 disappearances date at CDP in WY2006 for three forcing uncertainty scenarios and the Essery et
 1463 al. (2013) structural uncertainty.